

**Enabling Robotic Manipulation in Remote Environments
with Shared Autonomy**

by

Amy Phung

B.S., Olin College of Engineering, 2021

Submitted to the Department of Aeronautics and Astronautics
in partial fulfillment of the requirements for the degree of

Master of Science in Aeronautics and Astronautics

at the

MASSACHUSETTS INSTITUTE OF TECHNOLOGY

and the

WOODS HOLE OCEANOGRAPHIC INSTITUTION

June 2023

© 2023 Amy Phung. All rights reserved.

The author hereby grants to MIT and WHOI permission to reproduce and
to distribute publicly paper and electronic copies of this thesis document
in whole or in part to any medium now known or hereafter created.

Author Amy Phung
Joint Program in Oceanography/Applied Ocean Science and Engineering
Massachusetts Institute of Technology
and Woods Hole Oceanographic Institution
May 12, 2023

Certified by Richard Camilli
Associate Scientist of Applied Ocean Physics and Engineering, WHOI
Thesis Supervisor

Certified by Brian Williams
Professor of Aeronautics and Astronautics, MIT
Thesis Supervisor

Accepted by David Ralston
Associate Scientist with Tenure, WHOI
Chair, Joint Committee for Applied Ocean Science and Engineering

Accepted by Jonathan P. How
R.C. Maclaurin Professor of Aeronautics and Astronautics, MIT
Chair, Graduate Program Committee

Enabling Robotic Manipulation in Remote Environments with Shared Autonomy

by

Amy Phung

Submitted to the Department of Aeronautics and Astronautics
on May 12, 2023, in partial fulfillment of the
requirements for the degree of
Master of Science in Aeronautics and Astronautics

Abstract

The evolution of robotics technology continues to facilitate exploration and scientific study in remote environments, enabling research in areas that were previously impossible to reach. Robots operating in space and marine environments encounter similar operational challenges, as both face high operational costs, bandwidth-limited conditions, and natural, unstructured environments where dynamic obstacles might be present. Within the oceanographic domain, conventional deep-sea sampling operations involve remotely operated vehicles (ROVs) equipped with robotic manipulator arms to complete dexterous tasks at depth. While effective, deep-sea ROV operations require specialized instrumentation, highly trained shipboard personnel, and large oceanographic vessels, which make deep-sea samples inaccessible to most.

This thesis presents the SHared Autonomy for Remote Collaboration (SHARC) framework, and evaluates its utility within an oceanographic context. By leveraging shared autonomy, SHARC enables shore-side operators to collaboratively carry out underwater sampling and manipulation tasks, regardless of their prior manipulator operations experience. With SHARC, operators can conduct manipulation tasks using natural language and hand gestures through a virtual reality (VR) interface. The interface provides remote operators with a contextual 3D scene understanding that is updated according to bandwidth availability.

Evaluation of the SHARC framework through controlled lab experiments indicates that SHARC's VR interface enables novice operators to complete manipulation tasks in framerate-limited conditions (i.e., <0.5 frames per second) faster than expert pilots using the conventional topside controller. For both novice and expert users, the VR interface also increased the task completion rate and improved sampling precision. During sea trials, SHARC enabled collection of an underwater *in-situ* X-ray fluorescence (XRF) measurement at more than 1000 meters water depth in the Eastern Pacific with centimeter-level precision by remote scientists with no prior piloting experience. This demonstration provides compelling evidence of SHARC's utility for conducting delicate operations in unstructured environments across bandwidth-limited communications, which holds relevance for improving operations in other

sensitive domains where dexterity is required. SHARC's ability to relax infrastructure requirements and engage novice shore-side users provides a promising avenue for democratizing access to deep-sea research.

Thesis Supervisor: Richard Camilli

Title: Associate Scientist of Applied Ocean Physics and Engineering, WHOI

Thesis Supervisor: Brian Williams

Title: Professor of Aeronautics and Astronautics, MIT

Acknowledgments

I'd first like to express my gratitude to my advisor, Richard Camilli, for his encouragement and mentorship in helping me pursue my own research ideas, and for providing a wealth of knowledge and support to help bring them to fruition. Thank you for your unwavering support and guidance throughout my studies and for encouraging me to keep an open mind to new opportunities.

I'd like to extend my thanks to my colleagues in the Deep Submergence Lab, especially Naomi Czupryna, Casey Machado, Molly Curran, Victor Naklicki, Mike Jakuba, and Stefano Suman for their support. And to my former labmates Gregory Burgess and Peter Ventola, thank you for the warm welcome to WHOI, and for your guidance and advice. To my collaborators Matthew Walter, Gideon Billings, and Andrea Daniele, thank you for your insight, dedication, and support throughout our work together, and for helping me to become a better communicator, engineer, and scientist. I look forward to continuing to work with you all in the coming years.

To Brian Williams and MERS, thank you for welcoming me into your group, and for your company and mentorship. It's been a pleasure to join in your group meetings, and it's always fascinating to hear about all of your work with robotic planners and to talk about new ideas.

And most of all, I'd like to thank my family and friends for their love and support. To my Olin friends near and far, I'm always grateful for the spontaneous, yet insightful and interesting conversations we always have. To my friends at MIT and in the WHOI Joint Program, thanks for your friendship and for sharing my excitement when I ramble on and on about underwater robots and boats. And to my partner, Andrew, I'm grateful for your companionship all of these years - celebrating the successes, and staying with me through harder times, always being there as the voice of reason when I need it most. I'd especially like to thank my parents Lan Ngo and Hung Phung, and my sister Callie, for always encouraging me to dream big - through all these years of school thousands of miles from home, your love and support has always felt close.

This work was supported by funding from the National Science Foundation Graduate Research Fellowship under Grant No. 2141064 and the Ocean Engineering and Instrumentation Fellowship from the Link Foundation.

Contents

1	Introduction	15
1.1	Motivation for Robotic Intervention in Remote Environments	15
1.2	Limitations of Conventional Underwater Robotic Manipulation Operations	18
1.3	Challenges of Remote Operations	20
1.4	Autonomy in Remote Environments	20
1.5	Related Work on Human-Robot Collaboration Interfaces	22
1.6	Thesis Contributions	24
1.7	Thesis Organization	25
2	Proposed Shared Autonomy Framework	27
2.1	Introduction	27
2.2	Shared Perception	28
2.3	Shared Autonomy	31
2.4	Distributed Network Architecture	32
2.5	User Interfaces	33
2.6	Discussion	35
3	<i>In-Situ</i> Analysis with Field-Portable Instrumentation	39
3.1	Scientific Motivation & Challenges	39
3.2	Case Study: X-Ray Fluorescence	40
3.3	Results: Field deployment in San Pedro Basin, CA	43
3.4	Discussion	45

4 Democratizing access to the deep-sea	51
4.1 Introduction	51
4.2 Experimental Validation: User Study	53
4.2.1 Participants	54
4.2.2 Experimental Setup & Testing Procedure	54
4.2.3 Results	58
4.3 Discussion	64
5 Discussion and Future Work	69
5.1 Contributions	69
5.2 Future work	70
5.2.1 Robust Perception in Turbid Conditions	70
5.2.2 Improved Control Methods	71
5.2.3 Adapting to Dynamic Obstacles	71
5.2.4 Integration on Multi-Manipulator Systems	72
5.3 Conclusion	72

List of Figures

1-1	Photo of an ROV pilot operating an ROV manipulator arm from an onboard control room with the conventional topside controller. Conventionally, pilots complete dexterous sampling tasks using this controller with support from numerous telemetry and video feeds. (Image credit: Matthew Walter)	19
2-1	Illustration of key components within the SHARC Framework. Vehicle data (e.g., camera feeds, manipulator joint position feedback) is sent via satellite communications from the ship to shore-side server which handles the distribution of data to remote users.	29
2-2	SHARC relies on shared perception between humans and robots to maximize capabilities and robustness during operations. Tool detection, vehicle model updates, and 3D scene reconstructions are handled by the automated system, and human input is used for interpreting video feeds and selecting sampling sites.	30
2-3	The SHARC-VR (a,b) and SHARC-desktop (c) interfaces enabled remote scientists to collect XRF and push core samples during sea trials in September 2021. The desktop interface screenshot includes annotations highlighting SHARC's key features, which are also present in the VR interface.	34

2-4 Mixed-reality view illustrating the revised SHARC-VR interface after field operations. In the participant’s view during user testing, the blue background was replaced with a real-time view of the participant’s physical environment to minimize their risk of bumping into walls/furniture.	36
3-1 $1/e$ attenuation lengths in water, by wavelength based on data from the National Institute of Standards and Technology (NIST) [Hubbell and Seltzer, 1995], The Center for X-ray Optics (CXRO) [Henke et al., 1993], and D. J. Segelstein’s Masters’ thesis [1981]. Attenuation lengths for wavelengths corresponding to the keV range for our XRF probe (2-50 keV) are highlighted. Visible light wavelength range is highlighted for reference. Figure adapted from Skoglund Lindberg [2010]	42
3-2 Using SHARC, we conducted <i>in-situ</i> XRF analysis in San Pedro basin at 1000 m water depth. This snapshot a representative video frame that is broadcasted to shore-side users with SHARC during measurement.	44
3-3 Illustration of the sampling process with SHARC. Remote scientists (green) using SHARC-VR (headset icon) and SHARC-desktop (monitor icon) collaborated with the onboard crew (blue) to take an XRF measurement and push core sample of a microbial mat within the San Pedro Basin.	46
3-4 XRF spectra measured in real-time indicated elevated iron concentrations in the microbial sample (red) above ambient (blue). A 10 minute integration time for each sample was used with the X-ray source operating at 15 kV and 15 μ A.	46
4-1 Photo of the conventional topside controller used to control the hydraulic manipulator arm during user testing	55

4-2	The in-air testbed used for user study consists of a hydraulic manipulator equipped with a basket for tools and samples, and can be configured to simulate a sample retrieval task (a) or a push-core sampling task (b). (c) The manipulator, camera, tool basket, and workspace position on the testbed (colored) closely resemble those on the physical vehicle (displayed in monochrome, for reference)	56
4-3	Illustration of the testing layout for the comparative user study. Participants gained familiarity with the conventional topside controller in the “training area” with direct line-of-sight to the physical arm (a), but operated the controller and the SHARC-VR interface in a separate room during testing (b).	57
4-4	(a) Frequency of trial outcomes per test group. (b) <i>Task Completion Rate</i> (R_{FPS}) among test groups, expressed across framerates. Across most framerates, both pilots and novices had a higher <i>Task Completion Rate</i> with SHARC-VR than with the topside controller.	59
4-5	Plots of <i>Task Completion Times</i> $T_{i,FPS}$ for the block pick-up (a) and push core (b) tasks as well as the <i>Expected Task Times</i> $\mathbb{E}[T_{FPS}]$ (c) across framerate. A power and linear trend are fitted to the topside controller and SHARC-VR data, respectively. The 2σ distribution of points at each framerate is shaded in (c). At decreased framerates, pilots and novices complete both the block pick-up and push core tasks quicker with SHARC-VR than with the topside controller. This difference is more pronounced among the <i>Expected Task Times</i> , which factors in the <i>Task Completion Rate</i>	61
4-6	<i>Expected Task Times</i> $\mathbb{E}[T_{trial}]$ for the block pick-up task plotted by trial number. Initial and final trials are conducted at 10 FPS to control for framerate. SHARC-VR times exhibit a slight negative correlation with trial number independent of framerate, while topside controller times appear to be framerate dependent.	62

- 4-7 Map of push core placement locations by test group relative to the target center. Confidence ellipses (2σ) are shown for each group. For both pilots and novices, push core locations achieved using the SHARC-VR formed a tighter confidence ellipse than those with the topside controller. 63
- 4-8 Visual illustration of the supported framerates for the underwater communication methods listed in Table 4.4. The maximum framerate with communications across the conventional tether or light fiber is limited by the camera's hardware rather than the communication method. 67

List of Tables

2.1	List of features developed for each version of the SHARC interfaces. Experiences with the VR interface during field operations informed improvements to the interface to increase usability among novice users.	35
4.1	Number of participants in each of the four user study test groups, which consisted of ROV pilots and novices using the topside controller and SHARC-VR interfaces. Some participants tested both interfaces, and thus are in two different test groups.	54
4.2	Absolute and relative improvements in <i>Expected Task Time</i> $\mathbb{E}[T_{\text{trial}}]$ for each test group between the initial and final block-pickup trials. The absolute and relative improvements were smaller with the SHARC-VR interface than with the topside controller for both pilots and novices.	62
4.3	Ensemble accuracy and precision of push core placement per test group. On average, users demonstrated greater precision with SHARC-VR than with the topside controller. Pilots using SHARC-VR exhibited the highest accuracy across all test groups.	63
4.4	Estimated frame update rates with various underwater communication methods, computed based on bandwidth limitations reported by Bowen et al. [2013]. Framerate estimates assume standard-definition (SD) resolution (640 x 480 px) from 2 camera feeds. The listed times (min:sec format) are based on the <i>Expected Task Time</i> from the nearest recorded framerate illustrated in Figure 4-5c.	66

Chapter 1

Introduction

1.1 Motivation for Robotic Intervention in Remote Environments

The human drive to explore and comprehend the world around us has been an enduring trait since prehistoric times, with early explorers searching to discover untouched lands, uninhabited islands, and untapped resources. Today, the frontier of exploration has shifted to the remote and hazardous environments of deep space and the abyssal sea floor. Despite the exorbitant cost, we have developed methods to facilitate exploration in these remote environments through the use of specialized equipment such as space suits and human-occupied submersibles. However, there is a growing trend towards using robots as proxies for human exploration in these environments [Wong et al., 2018]. On Earth, robots have played a crucial role in the study of chemosynthetic microbes near hydrothermal vents, which fundamentally challenged the prior scientific belief that all life on Earth derived from photosynthesis [Corliss et al., 1979; Ballard and Hively, 2017]. In space, robots have enabled the discovery of oceans beneath ice caps on other ocean worlds [Lunine, 2017], traces of past rivers, streams, and lakes on Mars [Witze et al., 2022], and methane lakes on Titan [Stofan et al., 2007]. Using robotic vehicles to continue to push the limits of exploration has proven to be transformative, enabling us to access and study environments that were

previously impossible to reach.

Robotic exploration vehicles can broadly be classified into two classes: observation vehicles and intervention vehicles. Both classes of vehicles are used to collect environmental data and measurements, but intervention vehicles are additionally equipped with robotic manipulator arms capable of completing dexterous tasks. This additional dexterity permits them to achieve a greater degree of physical interactions with the environment, which necessitates care during operations to minimize environmental disturbance. Meanwhile, preliminary, high-coverage data collection is often conducted by observation vehicles. For example, fly-by satellites are used to photograph the surface of the moon [Kopal, 1966] and autonomous underwater vehicles (AUVs) are used for benthic-scale seafloor mapping on Earth [Williams et al., 2010]. However, intervention vehicles are required for precise *in-situ* sampling that cannot be completed without direct contact with the surface. In space, the Mars Rover Perserverence uses robotic manipulator arms to collect *in-situ* samples with instrumentation such as the Planetary Instrument for X-ray Lithochemistry (PIXL) probe, which employs a contact switch to hold the sensor at a precise offset from the Martian surface [Allwood et al., 2015]. On Earth, robotic manipulators on human-occupied vehicles (HOVs), remotely operated vehicles (ROVs), and hybrid remotely operated vehicles (HROVs) are utilized to sample plumes [Reddy et al., 2012], collect geologic samples [Paull et al., 2001], and retrieve biological specimens from the seafloor [Bünz et al., 2020]. The development of intervention-capable AUVs (I-AUVs) shows promise in increasing the capabilities of underwater robotic manipulators [Ribas et al., 2011], but further testing in unstructured environments is required before I-AUVs can be deployed for regular operational use. As these examples illustrate, advancements in robotics technology have improved the capabilities of exploration and greatly reduced the barriers to accessing remote environments.

Answering scientific questions about Earth or other planetary bodies often require highly interdisciplinary teams comprised of multiple researchers, each with their own individual research goals. Due to the significant expense and labor required for field data collection, robotic deployments frequently strive to address a wide variety of

scientific objectives, which requires the coordination of various operations on a short timeline. For instance, ocean observing systems composed of a multitude of coordinated observation assets such as deep-sea buoys, ROVs, autonomous gliders, shipborne sensors, and remote sensing technologies require close coordination to achieve their scientific goals [Vrolijk et al., 2021; Isern and Clark, 2003]. In order to facilitate this coordination, prior work has leveraged satellite-based internet access to support collaborative frameworks [Gancet et al., 2015] and remote telepresence technologies [Martinez and Keener-Chavis, 2006], which enable participants to engage with each other in the simultaneous development of scientific understanding and operational plans. The development of these technologies must prioritize intuitive and user-friendly design to enable scientists to remain fully engaged in their research without undue distraction caused by the technology's complexity. By understanding how humans interact with robots, designers can optimize human-robot interfaces to be more intuitive and efficient for people to operate. Human factors research has helped to facilitate trust on human-robot teams [Khalid et al., 2016], increase their operational capabilities [Hopko et al., 2022], and reduce the learning curve of operations [Goza et al., 2004].

The evolution of exploration robotics technology continues to be propelled by scientific needs and research objectives. While space and ocean robots encounter similar operational challenges, there exists a pressing need to improve robotics technology specifically for oceanographic research. The ocean plays a crucial role in circulating heat, water, carbon, and nitrogen, which are all essential for terrestrial life and drive global weather patterns that have direct implications for human society. We also rely on the oceans as a rich source of natural resources, including oil and gas reserves, minerals, and renewable energy sources such as wind and wave power. Beyond its physical properties, the ocean also contains the largest ecosystem on the planet, yet it's one of the least explored and understood regions on Earth [Ramirez-Llodra et al., 2010]. Thus, making advancements in ocean exploration technology is essential for increasing our understanding of the intricate interplay between Earth's natural processes and human activities.

1.2 Limitations of Conventional Underwater Robotic Manipulation Operations

Currently, dexterous sampling tasks at depth are performed by ROVs equipped with robotic manipulator arms. ROV pilots directly teleoperate these manipulators with a topside controller in a shipborne control room containing numerous video and telemetry data displays [Hegde et al., 2015], as illustrated in Figure 1-1. However, teleoperation has several limitations that compromise the effectiveness and efficiency of the tasks being performed. First, it places significant cognitive load on the operator, who must reason over both the high-level and low-level objectives simultaneously. For instance, operators must select an optimal sample site based on available data, while constructing a 3D scene understanding from 2D camera feeds and determining arm motions required to achieve the necessary end-effector pose for sampling. Second, operators typically exercise one joint angle at a time in a “joint-by-joint” teleoperation mode when using conventional control interfaces [Pilarski et al., 2012], which restricts dexterity, limits efficiency, and can be error-prone when operating over a time-delayed, bandwidth-constrained channel [Thobbi et al., 2011]. Thus, conventional ROV operations require a high-bandwidth, low-latency tether, which restricts the ROV’s maneuverability, limits its vertical and lateral range, and increases the infrastructure requirements [Bowen et al., 2013]. Despite these limitations, direct teleoperation is still the standard approach for benthic sampling with ROVs [Jamieson et al., 2013].

Unfortunately, access to ROVs for sampling remains prohibitively expensive for many researchers since their operation requires a surface support vessel (SSV) with a highly trained operations crew, and SSV space constraints limit the number of on-board participants. Expanding shore-based access for remote scientists to observe and control robotic sampling processes can increase the number of scientists engaged in the deployment while reducing barriers to participation (e.g., physical ability, experience, or geographic location). However, the conventional direct-teleoperation approach is infeasible for remote operators due to the considerable bandwidth limitations and la-



Figure 1-1: Photo of an ROV pilot operating an ROV manipulator arm from an onboard control room with the conventional topside controller. Conventionally, pilots complete dexterous sampling tasks using this controller with support from numerous telemetry and video feeds. (Image credit: Matthew Walter)

tency inherent in satellite communications, and thus some degree of ROV autonomy is required [Bowen et al., 2008]. By offering a collaborative approach that blends human expertise with machine capabilities, shared autonomy has the potential to improve the efficiency and effectiveness of operations by bridging the gap between direct teleoperation and full autonomy as the research progresses.

1.3 Challenges of Remote Operations

Communication with robots in ocean and space environments presents significant challenges and is often intermittent, high in latency, and extremely limited in bandwidth, which in turn requires robots to be capable of operating with minimal human supervision to be effective. For certain tasks, such as under-ice surveying [Crees et al., 2010] or cave mapping [Mallios et al., 2016], the robot must be capable of operating beyond the range of physical tethers. In these scenarios, full autonomy is required when the vehicle is submerged since communication is typically only possible when the vehicle is at the surface or near a support vessel. Even at the surface, the vehicle’s bandwidth for satellite communications is typically limited to a modest 10 Kbps with latencies on the order of seconds. In contrast, the bandwidth available to the Mars Exploration Rover (MER) vehicles was over 10 times higher, but had significantly higher latency with up to 40 minute round-trip communication times [Bellingham and Rajan, 2007]. In either of these low-bandwidth, high-latency situations, controlling the robots with a high-frequency teleoperated control approach is infeasible, and thus greater onboard autonomy is required.

1.4 Autonomy in Remote Environments

Fully autonomous observation vehicles have been deployed in both marine and space environments. In 1999, NASA’s observation vehicle Deep Space 1 (DS1) demonstrated fully autonomous onboard decision-making capable of diagnosing and recovering from failures, and autonomous navigation processes which used images of stars to trian-

gulate its position during flight [Muscettola et al., 1998; Bhaskaran et al., 1996]. In marine environments, using fully autonomous vehicles for data collection is routine. For example, AUVs are used for seafloor surveys [Wynn et al., 2014], autonomous robotic profiling floats are used to collect measurements of the water column [Chai et al., 2020], and autonomous underwater gliders (AUGs) are used to study variations in the structure of the water column [Ratsimandresy et al., 2014].

The degree of autonomy that can be achieved in mobile exploration robots is highly dependent on the robustness of their perception systems, as these robots must reliably sense and interpret their environment to adapt to changes. In contrast to robots that operate in structured environments, such as manufacturing robots on a factory floor, exploration robots must operate in unknown environments with dynamic obstacles and disturbances. For instance, AUVs need to be capable of detecting rocks and changes in seafloor topography to avoid collisions [Houts et al., 2012]. Improvements in robotic perception can pave the way towards more complex autonomous processes, and consequently increase the capability of the robot. Ongoing work focuses on fielding robots capable of dynamic replanning based on environmental observations, from both a safety perspective and to maximize the probability of collecting scientifically useful data [Ayton, 2022].

There is a significant time and cost investment required for the specialized hardware, engineering effort, and operations support associated with deploying a robotic vehicle in space or in the ocean, and thus there is a substantial focus on robust practices when it comes to developing new autonomy processes. For interplanetary exploration vehicles, the software used during operations has deliberately been kept simple to minimize the probability of unexpected failures. In space, vehicles are typically controlled with predefined commands that are executed onboard with limited contextual awareness. While robust, this control method is inefficient and requires substantial human input to ensure the robot's safety. In the case of the MER vehicles, over 200 engineers were needed to support the vehicles 24/7 [Bellingham and Rajan, 2007]. Similarly, for ocean exploration, autonomous processes are also deliberately kept simple. AUVs are routinely directed to move to a specific waypoint or traverse

along predefined patterns [Miguelanez et al., 2010], and robotic profiling floats only control their depth while freely drifting with ocean currents for lateral movement [Chai et al., 2020].

While fully autonomous exploration vehicles have been deployed for observation missions, virtually none of these vehicles are capable of intervention. Although methods for autonomous underwater manipulation are advancing [Ribas et al., 2011], contextual awareness in unstructured environments remains insufficient for fully autonomous systems to operate reliably [Simetti, 2020]. Prior works have demonstrated fully autonomous manipulation processes, but these methods are often tested in controlled test tank environments where water clarity and dynamic obstacles are not an issue [Cieslak et al., 2015] or are used to manipulate objects with a known geometry [Palomeras et al., 2014; Prats et al., 2012]. In 2019, the first-known fully autonomous collection of a sample with a robotic manipulator arm in a natural underwater environment was conducted by Billings et al. [2022b], which still required pilot assistance for navigating the vehicle to the sample site beforehand. In space, the 2020 Perseverance Mars rover’s robotic manipulator can be position-controlled, but still requires human inputs from mission control on Earth for sample site selection and data analysis [Moeller et al., 2021].

1.5 Related Work on Human-Robot Collaboration Interfaces

Due to the risks associated with onboard deliberation processes, the adoption of fully autonomous systems by the operations and science communities has proceeded slowly [Bellingham and Rajan, 2007]. Until fully autonomous systems acquire sufficient heritage, uncertainties about their performance in novel situations present an undue risk to operations. Instead, an increasingly popular approach is to adopt mixed-initiative methods, which enable humans to aid the robot in its decision-making while delegating low-level computation and control tasks to the robot [Jiang and Arkin,

2015]. These systems provide a robust way for the operations and science communities to test recent developments in autonomy research while maintaining oversight before these methods have fully matured [Goodrich et al., 2001]. For instance, the Mixed-Initiative Activity Plan GENerator (MAPGEN) [Bresina et al., 2005] was employed for planning science and engineering activities for the MER vehicles. This system enabled scientists on Earth to plan science activities by specifying constraints on observations instead of focusing on low-level control of the hardware. Early tests with this system showed that using mixed-initiative techniques led to a 20% increase in the quantity of science data without compromising on the quality, which increased confidence in deploying the system [Bellingham and Rajan, 2007].

In the terrestrial domain, recent work has explored learning-based approaches to infer human intent in order to increase an autonomous system’s robustness to bandwidth limitations during remote teleoperation [Tanwani and Calinon, 2017]. For underwater manipulation operations, the DexROV project implemented a supervisory control system that could autonomously avoid joint limits and obstacles in the workspace, which enables remote users to control the ROV by sending end-effector motions via satellite communications [Birk et al., 2018]. While low dexterity tasks are now possible using autonomous underwater intervention systems in unstructured natural environments, improved modes for human-robot collaboration still hold promise for expanding operational capabilities [You and Hauser, 2012; Roncone et al., 2017] and increasing trust in human-robot systems [Billings et al., 2012]. User studies comparing novel VR interfaces to industry standard control methods found that VR reduced task completion times while also reducing the cognitive load for operators [Singh et al., 2013; Wonsick and Padir, 2020]. Even when the ROV control method is left unchanged, a recent study demonstrates that a 3D VR interface increases pilots’ sense-of-presence over a conventional 2D visual interface and reduces task completion time by more than 50% [Elor et al., 2021].

Similar to how interface improvements can reduce an operator’s cognitive load and task completion times, incorporating natural input modalities can further reduce cognitive demand. Due to their intuitive nature, using natural language (NL) and

gestures for succinct high-level, goal-directed control enables users to operate complex systems with little prior training. By decoupling human operator dexterity from manipulator control, NL also has the potential to increase task efficiency [Tellex et al., 2020], which is particularly beneficial in domains such as remote underwater manipulation which involve low-bandwidth, high-latency communication.

1.6 Thesis Contributions

The work described in this thesis aims to improve the capabilities of exploration robots in remote environments with the SHared Autonomy for Remote Collaboration (SHARC) framework, which leverages shared autonomy to distribute tasks between the robot and human operators based on their respective strengths. This framework enables real-time collaboration between multiple remote operators, who can issue goal-directed commands through free-form speech and hand gestures, and couples these natural input modalities with an intuitive 3D workspace representation. This thesis focuses on evaluating SHARC’s merits within an oceanographic context, and demonstrates its ability to enable shore-side scientists to contribute to deep-sea sampling operations without prior robotic manipulator operations experience.

The primary contributions of this thesis are summarized as follows:

1. Presentation of the SHARC framework
2. Demonstration of real-time *in-situ* analysis with delicate instrumentation by shore-side operators during field operations with SHARC
3. Evaluation of SHARC’s impact on increasing robustness to bandwidth limitations, reducing the operations learning curve, and improving task precision and efficiency

1.7 Thesis Organization

- Chapter 1 provides an overview of the motivation for and ongoing challenges associated with remote exploration
- Chapter 2 details the proposed shared autonomy framework and discusses design considerations and methodology
- Chapter 3 discusses challenges associated with scientific sampling with *in-situ* instrumentation and provides field results from SHARC-based operations
- Chapter 4 provides results from an in-depth user study with SHARC and discusses their significance for democratizing access to deep-sea research
- Chapter 5 concludes the thesis and provides recommendations for future work

Chapter 2

Proposed Shared Autonomy Framework

2.1 Introduction

The SHared Autonomy for Remote Collaboration (SHARC) framework facilitates collaboration between shore-side users and shipboard personnel. This framework adopts a distributed approach to allocate tasks between robots and teams of human operators based on their respective strengths, and promotes task parallelization among multiple simultaneous users to increase operational efficiency. By offloading low-level control and perception to the robot, SHARC enables users to focus on high-level sampling tasks and semantic understanding of the environment. This “shared autonomy” approach reduces the cognitive load on operators while lowering the probability of error in low-bandwidth conditions, which in turn enables shore-side users to actively participate in shipboard operations using consumer-grade hardware and a basic Internet connection regardless of their prior experience. SHARC’s reduced bandwidth requirement also facilitates real-time remote collaboration among shore-side users and enables it to scale to multiple simultaneous operations with additional operators and instrumentation.

SHARC users can participate as observers or as members of the operations team, which is subdivided into a technical and science team. Observers receive data streams

and the 3D scene reconstruction through one of SHARC’s interfaces, but are not authorized to issue manipulation commands. This mode of participation is designed to enable educators and other interested individuals among the general public to observe data through an interactive interface in real-time without requiring additional bandwidth on the ship’s satellite link. The technical team is responsible for operations support, which involves overseeing safety, managing communications, and delegating control authority. The science team operates payload instruments, generates task-level plans for sampling, and has one designated “science operator” who is authorized to control the manipulator.

The SHARC framework consists of four primary components: the ROS autonomy framework, the ship server, the shore server, and the shore-side user interface, as illustrated in Figure 2-1. The ROS autonomy framework handles the low-level manipulator control and machine perception processes, and accepts high-level commands as input. This framework runs on the ship server, which also enables onboard crew to control which data streams are transmitted to the shore server. The shore server distributes this data to the shore-side user interfaces, and handles authentication to ensure that only commands from the designated “science operator” are forwarded to the ship.

2.2 Shared Perception

Robots and humans each possess unique strengths when it comes to perception. Existing computer vision methods are capable of robustly estimating poses using visual fiducial tags [Kalaitzakis et al., 2021], and generating 3D scene reconstructions based on environmental features [Billings et al., 2022a]. Robots equipped with embedded sensors are able to locate their own joint positions within a fraction of a degree, and can plan and execute trajectories to maneuver around detected obstacles much faster than humans under certain circumstances.

Despite extensive efforts to program robots to be capable of handling increasingly complex situations, the uncertainty inherent to exploration makes it difficult

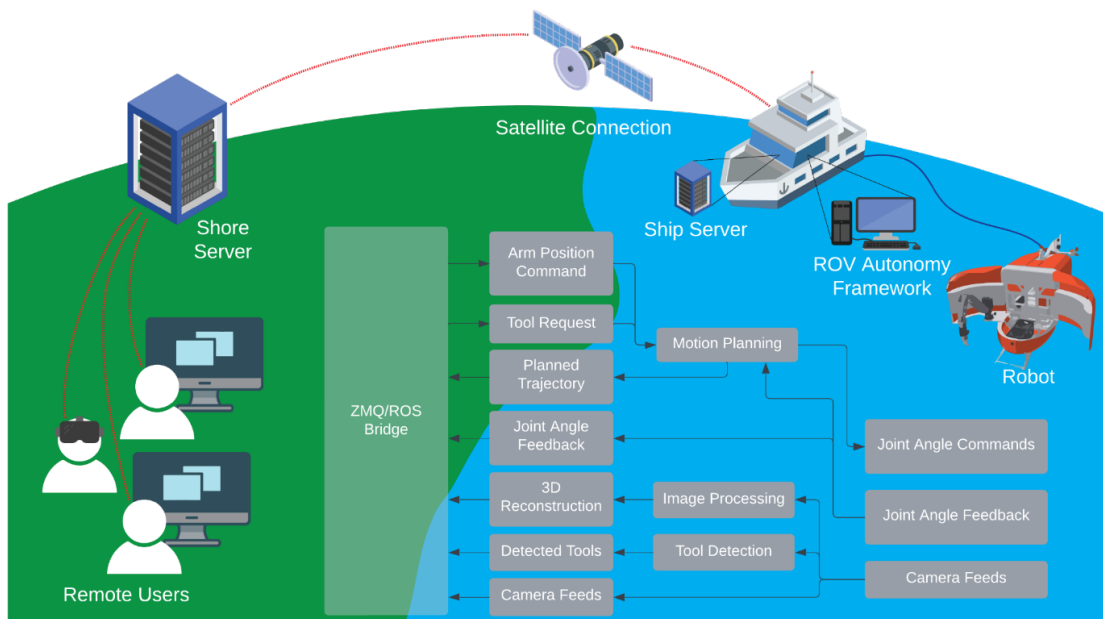


Figure 2-1: Illustration of key components within the SHARC Framework. Vehicle data (e.g., camera feeds, manipulator joint position feedback) is sent via satellite communications from the ship to shore-side server which handles the distribution of data to remote users.

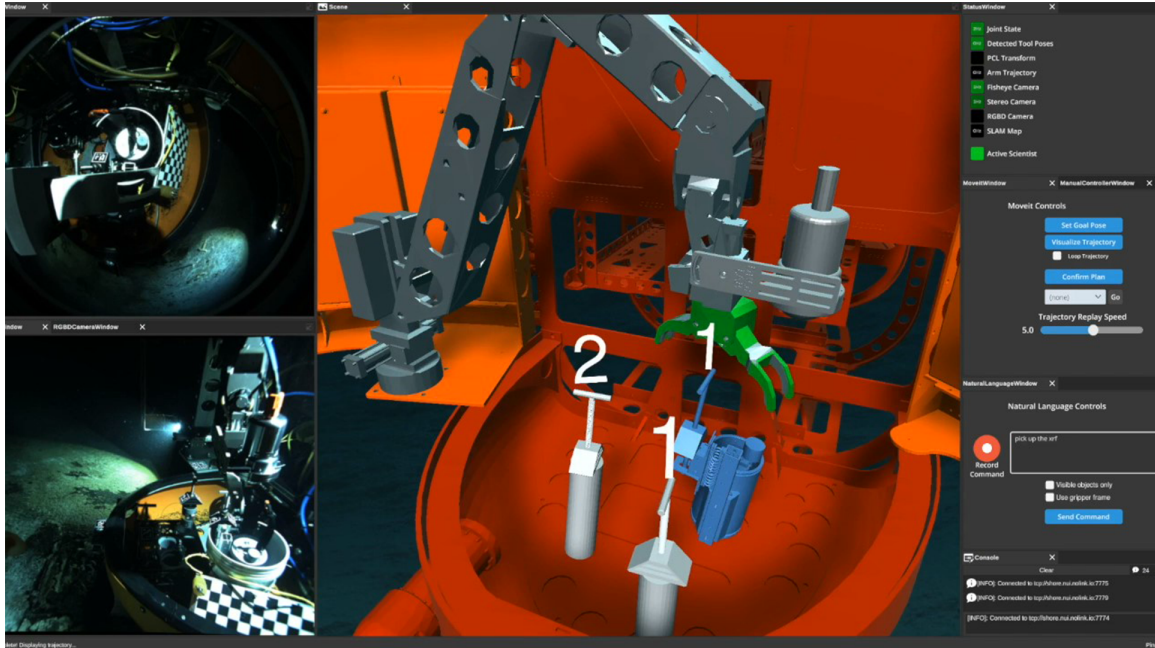


Figure 2-2: SHARC relies on shared perception between humans and robots to maximize capabilities and robustness during operations. Tool detection, vehicle model updates, and 3D scene reconstructions are handled by the automated system, and human input is used for interpreting video feeds and selecting sampling sites.

to robustly detect and adapt to all potential failures that may arise from unforeseen circumstances [Soares et al., 2018]. In the underwater domain, robots may encounter turbid conditions caused by transient currents that cause optical tracking systems to stop working, or featureless regions that result in sparse 3D reconstructions and poor localization. In these situations, humans can intervene and provide guidance when existing machine perception methods are inadequate. Since robust perception in unstructured environments remains challenging for robots [Simetti, 2020], the SHARC framework relies on shared perception to leverage humans' and robots' respective strengths (Figure 2-2). SHARC leverages machine perception to provide information such as tool location and type, construct a 3D scene reconstruction based on detected features, and display a model of its current configuration with respect to this scene reconstruction. Meanwhile, humans can provide a better semantic interpretation of the data and can select good sampling sites to achieve their scientific objectives.

Operations typically rely on human reasoning to interpret data in real-time and adapt sampling plans based on recent observations. In certain cases, automated

processes can also contribute to at-sea data analysis, particularly for pre-processing data [Rees et al., 2019], extracting data from datasets too large to sort through manually [Smith et al., 2022; McGillivray and Zykov, 2016], or supporting decision-making onboard autonomous vehicles [Laun, 2022]. Using automated processes to guide adaptive science can also be helpful since they can potentially find correlations between data or identify new sampling sites that may not have been obvious to humans [Vrolijk et al., 2021].

2.3 Shared Autonomy

Manipulator operations with the conventional topside controller require a reliable connection between the vehicle and the controller with sufficient bandwidth to support both the controller inputs ($\sim 100+$ Hz) and multiple real-time video streams ($\sim 15\text{-}20$ Hz) that visualize the workspace from multiple angles [Sivčev et al., 2018], which are not attainable with satellite communications. To enable manipulator control by shore-side operators, SHARC utilizes an autonomy framework to perform low-level trajectory planning and manipulator control. For our implementation, we used a ROS autonomy framework [Billings et al., 2022b] built on MoveIt [Chitta et al., 2012], and used AprilTags [Wang and Olson, 2016] for tracking the tool poses.

This framework also enables control of the arm via high-level objectives, which significantly reduces the bandwidth required for operations. With the automated tool detections, manipulator joint feedback, and known vehicle model, the vehicle can autonomously move the end-effector or place a tool at a specified pose without additional input from the user. In a quasi-static environment (i.e., obstacles can be considered stationary relative to manipulator dynamics), this pose request only requires one “frame” of data to inform the user about the vehicle and environment’s current state. In contrast, the conventional teleoperation approach can require upwards of 300 frames to complete a 30-second task with a 10 FPS update rate, which requires substantially more bandwidth to support. SHARC also automates routine tasks, such as tool pick-up and return. With a shared autonomy approach, these

tasks can be safely completed with three frames of data - one to capture the current workspace state, a second to confirm the tool has been grasped or returned, and a third to confirm the arm has been moved clear of the tool basket after the pick-up or return is complete.

2.4 Distributed Network Architecture

With SHARC, a distributed network architecture is used to optimize bandwidth and data prioritization (developed by Andrea F. Daniele [Phung et al., 2022]). For our implementation, the robot sends recorded data over a high-bandwidth fiber-optic cable to the ship’s server, which runs on a ROS-enabled shipboard computer. This computer runs additional ROS nodes to interface with the ROS autonomy framework and process the sensor streams into a continually updated 3D scene representation. To reduce the bandwidth needed on the ship-to-shore satellite connection, we convert ROS messages to Concise Binary Object Representation (CBOR) messages to reduce their size before transmitting them with the high-performance messaging library ZeroMQ [Hintjens, 2013]. The ship server sends data (i.e., planned trajectories, joint angle feedback, camera feeds, the 3D scene reconstruction, and tool detections) to the shore server through the satellite link, which then forwards this information to the remote on-shore users. To control the amount of data sent over this link, limits on data framerates and sensor streams can be set from the ship server.

Although these processes for data prioritization and robot autonomy are handled onboard the ship in our implementation, these processes could be run directly onboard the vehicle in a future iteration. An onboard process for data distribution and autonomy would eliminate the need for the high-bandwidth tethered communications, which in turn would enable the robot to communicate with a shore-side server directly.

The shore server authenticates remote users using pre-shared credentials to distinguish between members of the operations team and observers. The shore server also authenticates requests to ensure that only the current “science operator” can submit

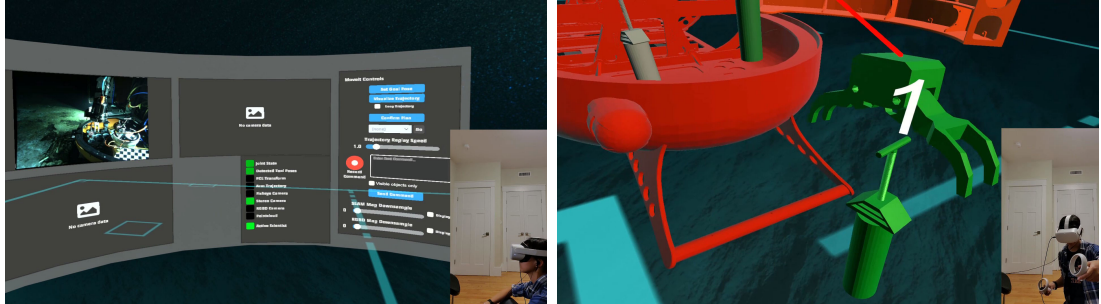
manipulator commands that are forwarded to the ship server. Members of the operations team can issue verbal high-level commands (e.g., “pick up the push core,” “move the arm forwards”). When parsing natural language commands, SHARC considers the current estimated environmental state to distinguish tools based on their relative positions (e.g., left or right) or tool type (e.g., push core or XRF). This shore server can also access resources that are difficult to access over the ship’s satellite internet connection, such as large datasets or machine learning models. In our implementation, the shore server uses cloud-based speech and natural language processing services for processing the verbal commands issued by operators.

2.5 User Interfaces

SHARC’s virtual reality (VR) and desktop interfaces display a model of the manipulator’s current pose with a 3D stereo reconstruction of the scene and 2D camera feeds in the background. Through interfaces, users can collaboratively identify target sample sites based on real-time data and defer low-level control of the manipulator to the automated system. Figure 2-3 illustrates the interfaces used during our field demonstration.

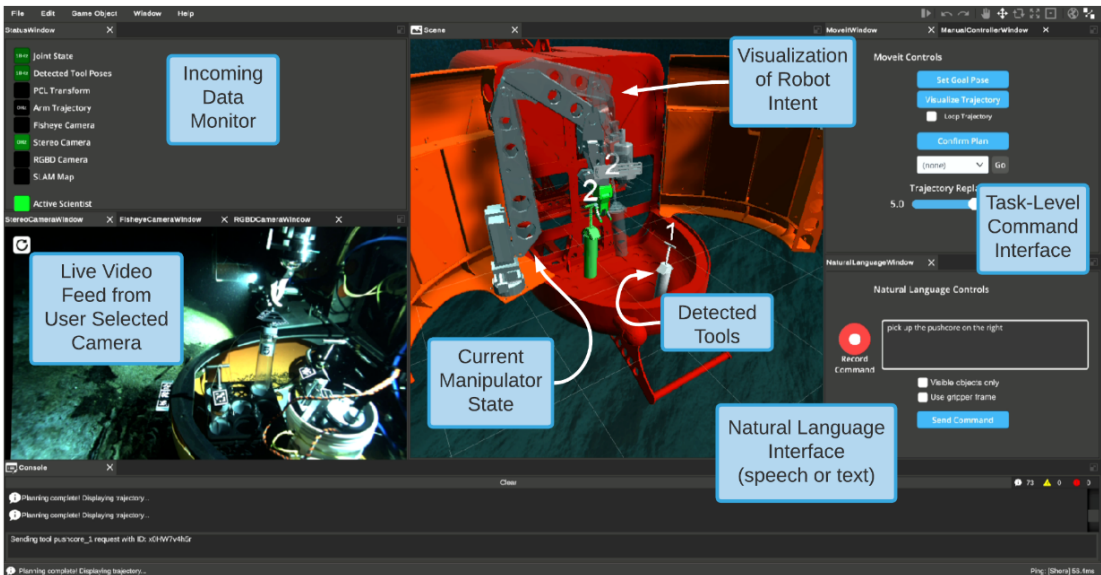
SHARC’s user interfaces are created with Unity (Unity Technologies; San Francisco, CA) for nontechnical end-users. Features of these interfaces are listed in Table 2.1. The desktop interface supports cross-platform operation, which was tested on Linux, Mac, and Windows machines. The VR interface only supported Windows and was developed and tested with an Oculus Quest 2 (Meta; Menlo Park, CA). No software development environment is needed for clients to use either of these interfaces.

Informed by our preliminary experiences with SHARC’s VR interface during field operations, we sought to improve the interface’s usability among novice users. With the original VR interface, the inability for users to see their physical surroundings during operations caused them to frequently run into objects around them. By adding passthrough augmented reality (AR), users were able to maintain awareness of their physical surroundings while using the interface. Users also found it difficult to memo-



(a)

(b)



(c)

Figure 2-3: The SHARC-VR (a,b) and SHARC-desktop (c) interfaces enabled remote scientists to collect XRF and push core samples during sea trials in September 2021. The desktop interface screenshot includes annotations highlighting SHARC's key features, which are also present in the VR interface.

Feature	Desktop	VR (Field Demo)	VR (User study)
3D workspace reconstruction	✓	✓	✓
Reachable workspace visualization	✓	✓	✓
Tool detection	✓	✓	✓
Automated tool pickup	✓	✓	✓
Live video feeds	✓	✓	✓
Manipulator position feedback	✓	✓	✓
Robot trajectory visualizer	✓	✓	✓
Inbound data monitor	✓	✓	
Speech interface	✓		
Hand tracking			✓
Gesture-based controls			✓
AR/passthrough mode			✓
Automated tool return			✓

Table 2.1: List of features developed for each version of the SHARC interfaces. Experiences with the VR interface during field operations informed improvements to the interface to increase usability among novice users.

rize all of the keybindings for the controller-based inputs, which in turn prompted us to replace the controllers with hand tracking and gesture recognition as an extension of the natural language interface. We also automated the tool return process in the revised interface after observing that users found it difficult to return the tools during operations. This revised interface (Figure 2-4) with passthrough AR, gesture-based inputs, and an automated tool return process was utilized during user testing.

2.6 Discussion

SHARC’s fundamental strategy for task allocation entails delegating responsibilities between the robot and operator based on their complementary strengths. Human operators are responsible for high-level scene understanding, goal selection (e.g., identifying sample locations), and task-level planning, which are challenging for existing perception and decision-making algorithms. These tasks are particularly difficult to automate in the unstructured environments typical of underwater science. Meanwhile, SHARC relegates the inverse kinematics, motion planning, low-level control, and obstacle avoidance processes to the robot, which helps to improve task efficiency

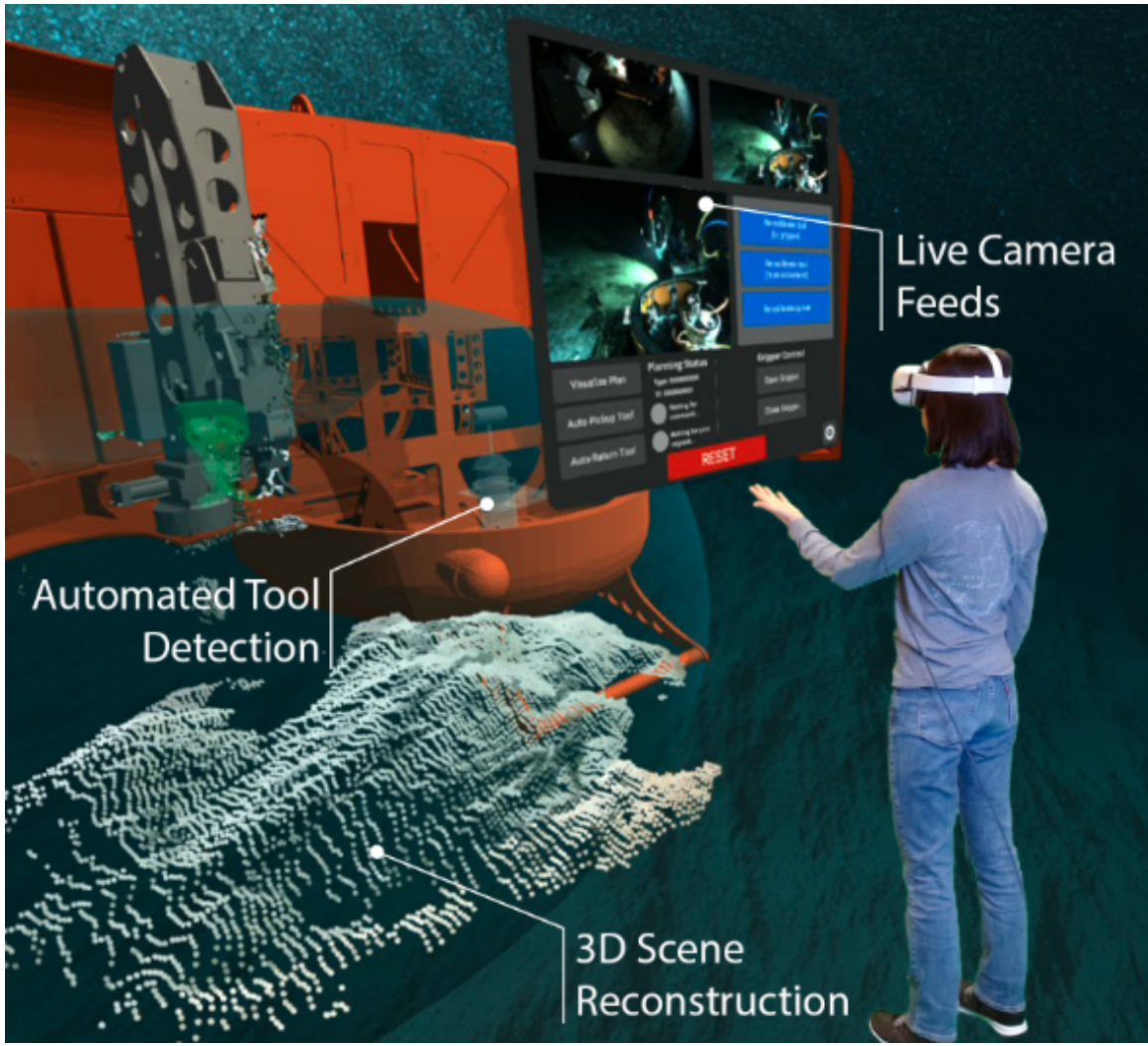


Figure 2-4: Mixed-reality view illustrating the revised SHARC-VR interface after field operations. In the participant's view during user testing, the blue background was replaced with a real-time view of the participant's physical environment to minimize their risk of bumping into walls/furniture.

[You and Hauser, 2012]. By rendering the robot’s intended actions in context of its current 3D scene understanding prior to execution, SHARC’s behavior is more predictable than contemporary interfaces such as the topside controller. With this task allocation approach, operators no longer need to simultaneously interpret the robot’s various high-frequency sensor streams while solving the low-level manipulator kinematics necessary to move the end-effector. Instead, these tasks are offloaded to the robot, which is designed to reduce operators’ cognitive load during operation.

Decreasing the cognitive load on operators also reduces the amount of training required for effective manipulator operations. The conventional topside controller interface typically used by pilots requires a substantial learning investment and is configured specifically for each manipulator arm model. Operators typically control manipulators in a joint-by-joint fashion, which requires them to constantly determine the joint angles necessary to achieve a desired end-effector pose. Acquiring proficiency in manipulator teleoperation is challenging because the high cost of infrastructure for underwater manipulation limits the time available for training on real hardware, and few training simulators that provide an effective alternative exist. To establish the situational awareness necessary to plan and control the manipulator, conventional teleoperation also requires operators to mentally construct a 3D scene from a variety of 2D camera feeds, which is particularly challenging when such feeds are low-resolution or framerate-limited. Environmental factors such as inadequate lighting, turbid conditions, and obstacles can impede visibility and obstruct areas of the workspace, which can increase the difficulty of the 3D scene reconstruction task. This cognitive load imparted on operators is exacerbated in domains like underwater intervention where inadvertent collisions with the environment and vehicle can be catastrophic.

SHARC expands upon DexROV’s supervisory control concept by facilitating real-time collaboration between multiple remote operators. In a manner similar to the approach taken by Zhao et al. [2019], which integrated elevation, LiDAR, and a photorealistic pointcloud generated by structure-from-motion (SfM) to produce an immersive VR view, SHARC provides a continually updated 3D scene representation

and real-time video feeds in either a desktop or VR interface. The SHARC desktop interface bears similarity to the web interface in [Gemmell et al., 2011], which enables users to visualize distributed coastal oceanography model and *in-situ* data across an internet connection. However, the SHARC interfaces improve upon these approaches by merging them to display data in a unified format and enable high-level control by remote users across an internet connection. Each user can also independently view the data from a unique perspective, which in turn increases the team’s collective situational awareness. By facilitating participation among multiple simultaneous remote users, SHARC can increase the robustness of operations and enable collaborative decision-making.

Inspired by the ways in which scientists communicate with ROV pilots, SHARC enables users to use natural language speech and gestures to convey high-level objectives to the robot. The inherent flexibility and intuitive nature of language enables users to succinctly issue complex commands that would otherwise be time-consuming and difficult to execute with conventional controllers. Within a matter of seconds, users can specify a task for the automated system that would take several minutes to complete with the conventional controller. In addition to reducing the cognitive load required of the operator, the intuitive nature of natural language and gestures minimizes the training required for operation and makes SHARC accessible to a diverse population of users. Future support for additional languages can enable users to communicate with the interface in their native language, which would further improve SHARC’s accessibility to users and decrease cognitive load. These natural input modalities also have the benefit of remaining functional under intermittent, low-bandwidth, and high-latency communication [Tellex et al., 2020], which helps SHARC enable participation from remote users.

Chapter 3

In-Situ Analysis with Field-Portable Instrumentation

3.1 Scientific Motivation & Challenges

In order to gain insights into the natural phenomena present in remote environments, scientists often rely on a variety of analytical instruments to study environmental variables such as temperature, pH, and elemental composition [Le Bris et al., 2001; Takahashi et al., 2020; Monk et al., 2021; Allwood et al., 2020; Tarcea et al., 2008]. While some of these analyses are conventionally conducted in laboratory settings, the development of field-portable methods for *in-situ* analysis has brought about significant advantages. The ability to monitor the data in real-time enables the results to guide decision-making in the field, which facilitates adaptive science that can enhance sample quality [Curtin et al., 1993]. *In-situ* measurement methods also generally incur a lower cost per sample, as the need for sample handling, transportation, and documentation is reduced [Camilli et al., 2004]. This, in turn, enables the collection of more samples, providing greater flexibility and coverage. Additionally, *in-situ* measurement methods avoid the potential compromise in scientific value of samples that may result due to changes in material state between collection and analysis [Camilli et al., 2004; Bertolini et al., 2021]. Maximizing the capabilities of field-portable instrumentation is especially important in planetary science, where preserving physical

samples for later lab-based analysis on Earth is challenging due to the limited payload space onboard vehicles, high cost of operation associated with flight systems, and strict planetary protection considerations [Muirhead et al., 2020; Bertolini et al., 2021; Craven et al., 2021].

Despite the benefits of *in-situ* operation, several challenges exist that must be addressed. One such challenge is that these instruments are often delicate and require a high level of dexterity to operate, which presents a significant obstacle for real-world use in remote environments where human dexterity cannot be relied on. Additionally, since these instruments can require precise positioning or direct contact with the environment [Le Bris et al., 2001; Takahashi et al., 2020; Allwood et al., 2020], extreme care must be taken during operations to prevent damage to the sensor or the environment.

3.2 Case Study: X-Ray Fluorescence

X-ray fluorescence (XRF), laser-induced breakdown spectroscopy (LIBS) [Takahashi et al., 2020], and Raman spectroscopy [Tarcea et al., 2008] are popular chemical analysis techniques among scientists since they are non-destructive methods that require little sample preparation. Among these, XRF works particularly well for detecting heavy metals, even if only trace amounts are present. Due to this, XRF has been widely used for applications ranging from monitoring lead levels in drinking water [Hołyńska et al., 1996], identifying annual boundaries in sediment cores for paleoclimate research [Alexandrin et al., 2018], identifying historical glazed paint techniques in archaeology [Hložek et al., 2017], and confirming meteoritic origins of ancient artifacts [Comelli et al., 2016]. For planetary science, astrobiologists are interested in studying the chemical composition of rocks on Europa and other planetary bodies since they may contain biosignatures or other clues of potential extant life [Figueroa et al., 2003; Hand et al., 2009; Kraft et al., 2018]. Thus, most Mars landers since 1976 have been equipped with an XRF instrument to make *in-situ* measurements of the chemistry of rocks and soils [Allwood et al., 2015].

Automating the XRF measurement process is challenging since the probe requires a precise distance between the sample and the instrument to accurately account for the distortion caused by the differential attenuation from the medium in which the measurement is taken in. In the case of the Planetary Instrument for X-ray Lithochemistry (PIXL) probe onboard the Mars rover Perseverance, the probe is coarsely positioned over the target site with a 6 degree-of-freedom (DoF) arm, and a physical contact switch is used to ensure a precise offset between the probe and the sample [Allwood et al., 2015]; however, this approach may be incompatible with compliant surfaces commonly found in marine environments, such as microbial mats and fine sediments. Taking *in-situ* XRF measurements underwater is especially challenging since the high attenuation rate of the X-rays in water requires the sensor to be in direct contact with the measurement surface. As illustrated by Figure 3-1, the attenuation distance for the XRF is on the order of millimeters, and thus even a slight offset between the tip of the probe and the surface can result in an indeterminate measurement. The high attenuation rate also increases the integration time required for each measurement in order to obtain an acceptable signal-to-noise ratio, and thus a rastering-based approach similar to one of PIXL’s operational modes [Allwood et al., 2015] would be impractical in underwater settings.

Conventionally, XRF analysis on marine sediment samples is conducted ex-situ on samples that are extracted by HOVs, ROVs, or gravity cores, and brought to labs onshore for analysis Smith et al. [1994]; Wien et al. [2005]. In terrestrial applications, the development of field-portable XRF analyzers enabled time and cost-efficient on-site analysis of environmental samples [Shefsky, 1997; Kalnicky and Singhvi, 2001]. In oceanography, the use of field-portable XRF analyzers for shipboard measurements on extracted cores brought about similar benefits, and provided timely results to guide on-site decision making [Stallard et al., 1995; Hahn et al., 2020]; however, since the samples are analyzed onboard the ship rather than in their original environment, these methods are still considered to be ex-situ. Prior experimental methods for underwater *in-situ* XRF measurements include lowering an XRF probe off the stern of a ship [Wogman and Nielson, 1980] and mounting an XRF on an AUV [Breen

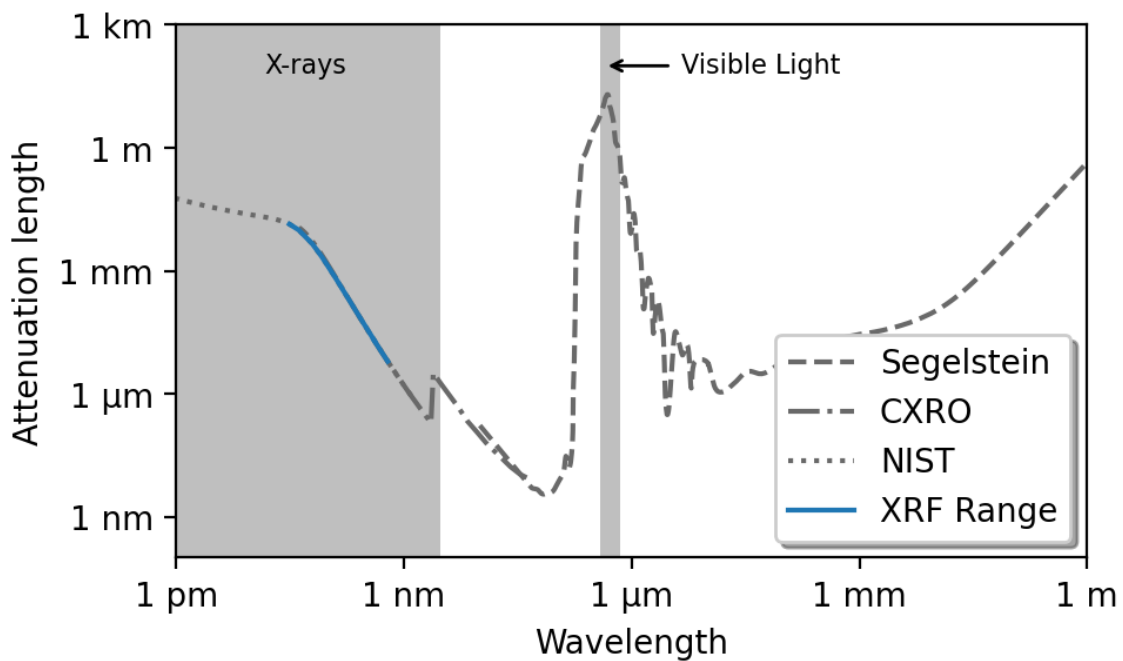


Figure 3-1: $1/e$ attenuation lengths in water, by wavelength based on data from the National Institute of Standards and Technology (NIST) [Hubbell and Seltzer, 1995], The Center for X-ray Optics (CXRO) [Henke et al., 1993], and D. J. Segelstein's Masters' thesis [1981]. Attenuation lengths for wavelengths corresponding to the keV range for our XRF probe (2-50 keV) are highlighted. Visible light wavelength range is highlighted for reference. Figure adapted from Skoglund Lindberg [2010]

et al., 2012], which limit the precision over sample site selection to kilometers and meters, respectively. Similar to Perserverence’s XRF measurement approach with PIXL [Allwood et al., 2015], we employ a high-DoF robotic manipulator to operate an underwater XRF probe. This approach enabled us to achieve centimeter-level precision using the probe during a field demonstration, which is discussed in the next section (Section 3.3).

3.3 Results: Field deployment in San Pedro Basin, CA

In September 2021, a team of remote operators distributed across the continental US (Chicago, Boston, and Woods Hole) conducted a dive operation in the San Pedro Basin of the Eastern Pacific Ocean with the SHARC-equipped Nereid Under Ice (NUI) vehicle [Bowen et al., 2014]. This shore-side team used SHARC’s VR and desktop interfaces to collaboratively collect a physical push core sample and record *in-situ* XRF measurements of seafloor microbial mats and sediments at water depths exceeding 1000 m, as illustrated in Figure 3-2.

The in-situ XRF sensor used during this demonstration is similar in design to the PIXL instrument [Allwood et al., 2015], and was developed for automated analysis of deep ocean sediments with robotic vehicles [Camilli, 2019]. This instrument is capable of detecting emission spectra from 2 to 50 keV at \sim 150 eV resolution, which corresponds to a detection range for elements with atomic weights ranging from Na through Zr. Laboratory-based underwater testing demonstrates that the instrument is capable of observing elements in the 2-50 keV spectral range, with minimum limits of detection in the ppm range using integration times on the order of minutes. Direct contact between the tip of this instrument and the sample is required, as even a slight offset of a couple millimeters can result in an unsuccessful measurement due to the extreme attenuation rate of X-rays in water (Figure 3-1). With this high attenuation rate and relative uncertainty in distance from the instrument’s X-ray window to the

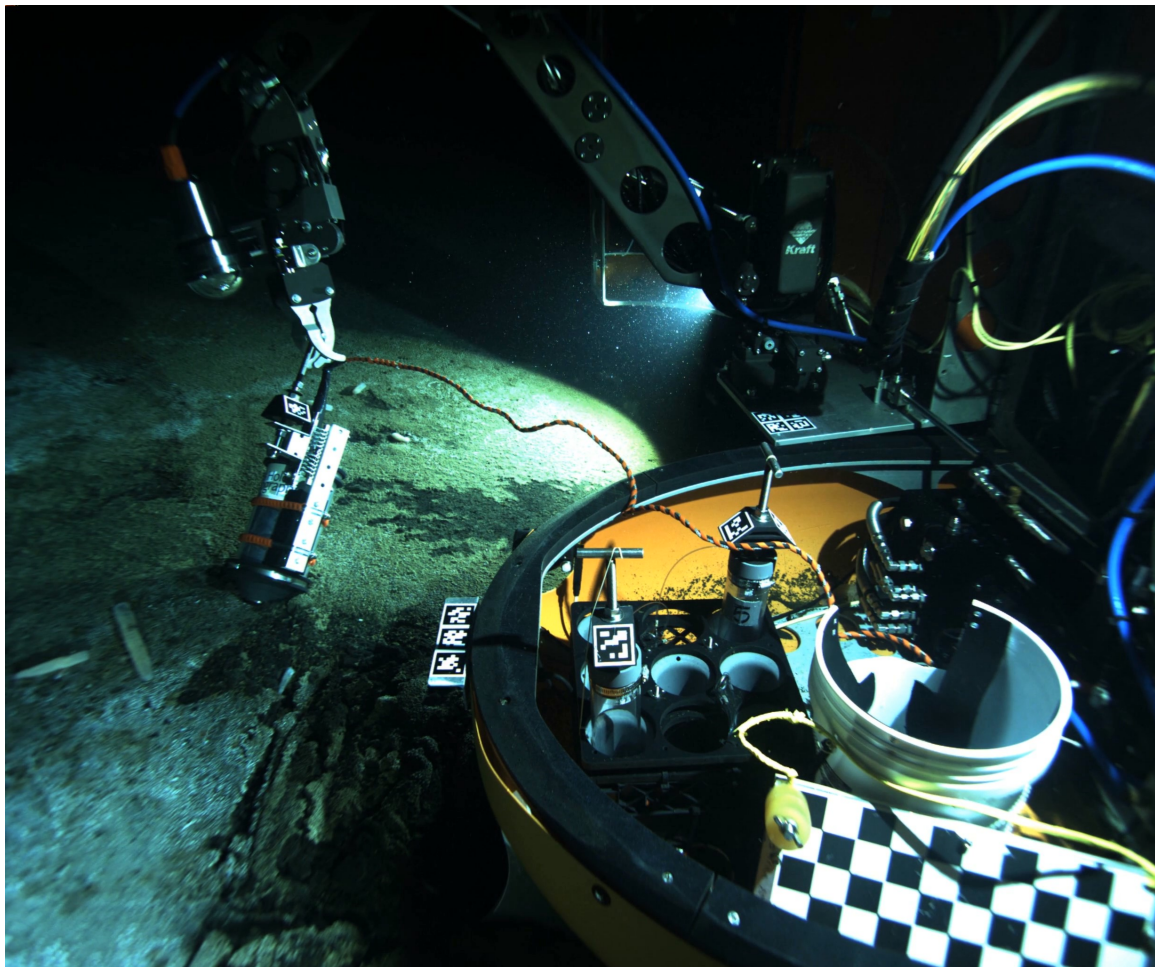


Figure 3-2: Using SHARC, we conducted *in-situ* XRF analysis in San Pedro basin at 1000 m water depth. This snapshot a representative video frame that is broadcasted to shore-side users with SHARC during measurement.

target, absolute estimates of elemental concentration were not possible *in-situ*.

During our field demonstration, we used a 10 minute integration time for each sample with the X-ray source operating at 15 kV and 15 μA . With SHARC, the science team maintained the XRF in direct contact with the seafloor with centimeter-level positioning precision during sample acquisition, thereby reducing environmental disturbance to the work site, minimizing the attenuation and distortion of the measurement, and improving upon the meter-level precision of prior underwater *in-situ* XRF measurement methods.

Figure 3-3 illustrates the *in-situ* XRF measurement process using SHARC. Although the remote science team was located more than 4,000 km away from the ship and relied on a low-bandwidth connection, SHARC enabled the team to sample visually distinct areas of the seafloor within and around a microbial mat. Real-time feedback from SHARC enabled active tuning of the XRF X-ray source and sensor integration parameters to maximize the signal-to-noise ratio while the sample was being collected. The XRF spectra (Figure 3-4) revealed elevated concentrations of iron within the microbial mats, which suggested the presence of chemolithoautotrophs, (e.g., *T. ferrooxidans*) [Stal, 1994]. In order to independently determine the presence of these microbes, the remote science team then collected a physical push core sample from the same microbial mat with SHARC.

3.4 Discussion

During our field trials, SHARC enabled us to achieve the first-known *in-situ* measurement with an X-ray Fluorescence (XRF) sensor and push core sample collected by a team of shore-side scientists [Phung et al., 2022], which provides compelling evidence of SHARC’s utility for conducting delicate operations in unstructured environments across bandwidth-limited communications. The implications of this technology could extend to other sensitive domains where dexterity is required, such as nuclear decommissioning [Pohl et al., 2020], deep space operations [Babarahmati et al., 2021], unexploded ordnance and disposed military munition remediation [F. Morrison et al.,

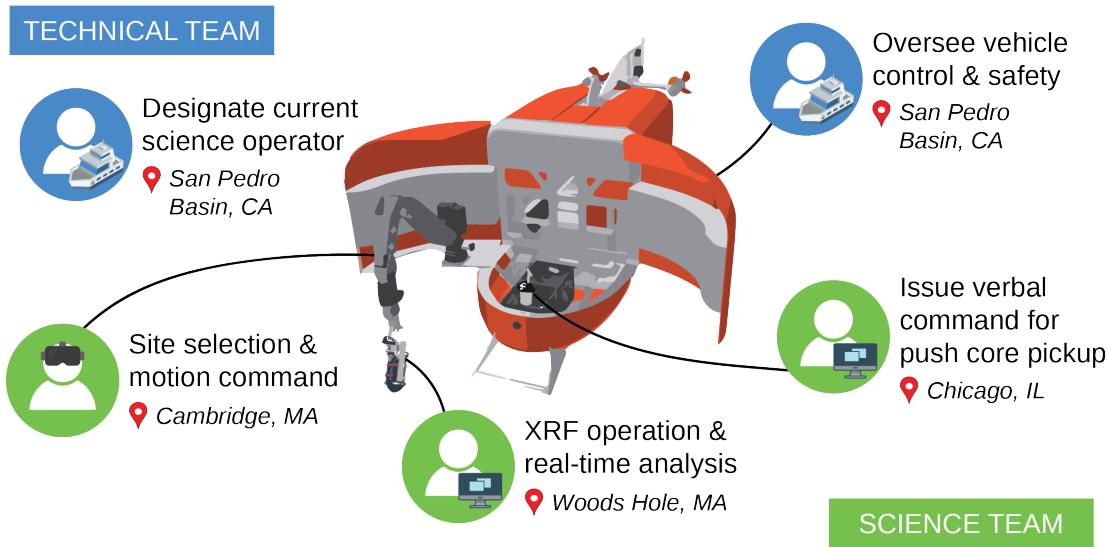


Figure 3-3: Illustration of the sampling process with SHARC. Remote scientists (green) using SHARC-VR (headset icon) and SHARC-desktop (monitor icon) collaborated with the onboard crew (blue) to take an XRF measurement and push core sample of a microbial mat within the San Pedro Basin.

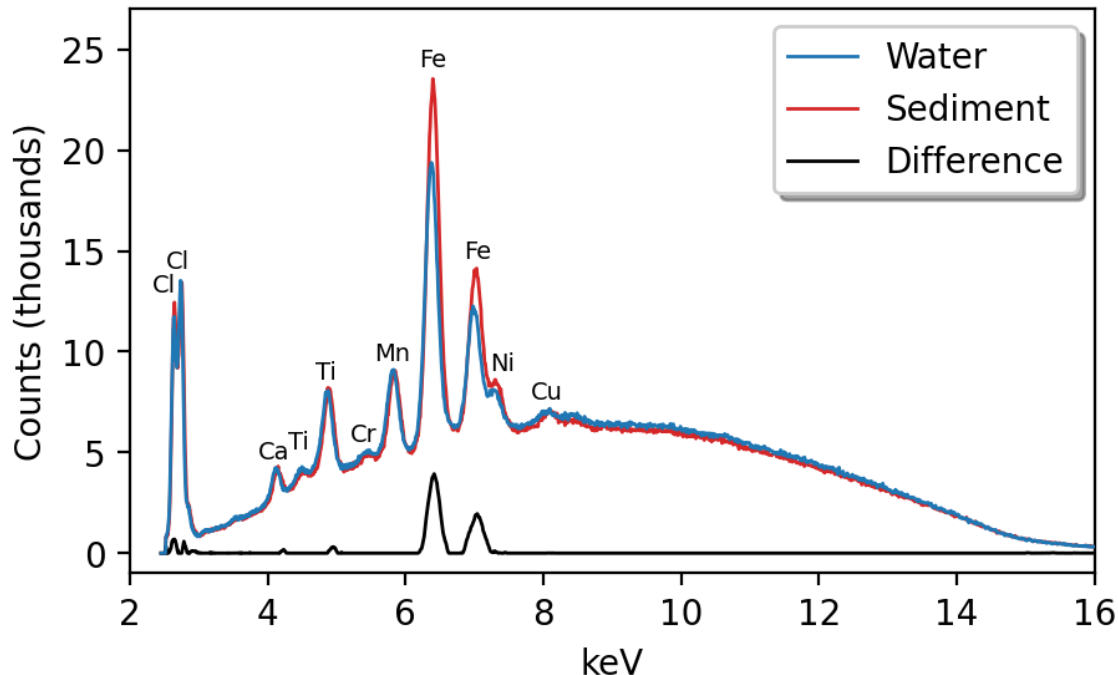


Figure 3-4: XRF spectra measured in real-time indicated elevated iron concentrations in the microbial sample (red) above ambient (blue). A 10 minute integration time for each sample was used with the X-ray source operating at 15 kV and 15 μ A.

2002], and search and rescue missions [Settimi et al., 2014]. Each of these applications pose their own unique set of challenges, and may impose bandwidth constraints on communications due to radiation, distance, or lack of communications infrastructure in the operational region. Despite the operational challenges, the consequences of failed manipulation tasks in these critical areas can have catastrophic effects on human health and safety, and thus robustness is paramount. In Chapter 4, we present compelling data that demonstrates SHARC’s ability to significantly reduce the probability of failure in low-bandwidth conditions, which can be instrumental for improving operational robustness in these high-stakes applications.

SHARC’s reduced bandwidth requirement also facilitates real-time remote collaboration among shore-side users and enables it to scale to multiple simultaneous operations with additional operators and instrumentation. For instance, in our demonstration, one scientist operated the *in-situ* XRF instrument and analyzed its data in real-time while another scientist simultaneously planned manipulator trajectories to potential push core sites. Although our demonstration focused on these two sampling methods, the ability to parallelize sampling tasks and data analysis can increase operational efficiency and tempo of sampling operations with other instrumentation as well. Parallelization also decreases the cognitive load on operators since tasks are distributed among several different people. This improves upon conventional ROV operations, which typically involve one pilot operating the arm for their entire shift.

SHARC’s ability to involve remote users during operations also allows for more flexible team configurations, which can improve operations in a variety of ways. In our field trials, the ability to involve remote users became particularly important during the COVID-19 pandemic when space onboard research vessels was especially restricted. Using SHARC, our entire team was able to contribute during sampling operations in the field, even though some team members were remotely located thousands of kilometers away on shore. SHARC’s ability to distribute tasks to a wide variety of shore-side operators also enables specialists to contribute their domain-specific knowledge to ship-based operations without needing to be physically present, which can be particularly useful for operating specialized sampling equipment or re-

ceiving advice from scientists with subject-matter expertise. Shore-side operators can also access resources that would be difficult or infeasible to access over the ship’s satellite internet connection. During our field demonstration, our shore-side team used cloud-based natural language processing services, which would have been expensive and time-consuming to use onboard the ship.

On Earth, the ability to remotely operate exploration vehicles in unstructured environments brings us closer to better understanding the frontiers of our planet. One of the Earth’s last frontiers lies underneath large ice sheets, which remain challenging to study with today’s technology. The conventional approach to under-ice research involves drilling boreholes to collect water samples and deploy sensors under the ice [Johnsen et al., 2001; Paterson, 1983]. More capable under-ice exploration vehicle designs consist of AUVs [Kunz et al., 2008] and AUGs [Duguid and Camilli, 2021] for observation and HROVs [Bowen et al., 2014] for intervention, both of which require high degrees of autonomy to cope with the communications challenges inherent to under-ice study. In planetary science, the ability to operate vehicles remotely is especially important as it is often impractical, if not impossible, to send people to conduct research on other planetary bodies. For example, factors such as space radiation, hostile environments, and distance from Earth pose hazards to astronaut health, which make human deep-space exploration missions unattainable with existing technology [Szocik and Braddock, 2019]. Instead, robots such as deep-space satellites are often used as proxies for humans in space exploration, and require higher degrees of autonomy since communication back to Earth is often unreliable [Turan et al., 2022]. For robots operating on planetary bodies closer to Earth, such as the Mars rover Perseverance, a human-in-the-loop control approach with automated subroutines is often used [Ebadi et al., 2022].

When operating in bandwidth-constrained environments, robots must possess greater autonomous capabilities, but iterative testing of autonomous processes for exploration robots is challenging due to the substantial cost of such operations. Consequently, operations involving exploration robots must balance the scientific merit of its actions with their probability of failure, and thus “correct-by-construction” ap-

proaches for autonomy are often used to ensure a high degree of operational robustness [Ceballos et al., 2011]. Technological developments in the field of planetary science heavily rely on testing in Earth-analog environments [Schuster et al., 2020], and in controlled testing environments for earlier-stage research [Muñoz et al., 2023]. In the case of autonomous underwater manipulation, some recent works have achieved full autonomy in controlled test environments, but remain limited to operations in structured environments with good water clarity (as discussed in Chapter 1 Section 1.4). The level of spatial precision required for operating delicate instrumentation is currently only achievable with human piloted robotic manipulators. Robust robotic perception and control remains challenging, but holds the promise of automating delicate, high precision *in-situ* measurement processes without the need for low-level human control and incumbent high-bandwidth connection. Full automation of *in-situ* sampling processes with underwater manipulators would enable us to someday use delicate instruments like the XRF to study oceans on Europa, Enceladus, and other planetary bodies with a similar level of spatial precision as the PIXL system onboard the Mars rover Perseverance [Allwood et al., 2020]. But until fully autonomous methods acquire sufficient robustness for such operations, using SHARC and other shared autonomy approaches can help to bridge the gap between direct teleoperation and full autonomy.

Chapter 4

Democratizing access to the deep-sea

4.1 Introduction

Deep-sea exploration is expensive, often requiring specialized instrumentation, highly trained personnel, and large oceanographic vessels, and as a result only a tiny fraction of the seafloor and the water column has been mapped and studied [Ramirez-Llodra et al., 2010; Teague et al., 2018; Thorsnes et al., 2020]. Although access to the deep sea remains a challenge, we rely on the oceans for regulating the Earth’s climate, water cycle, and carbon dioxide levels, and for renewable (e.g., wind and thermal energy [Ishaq and Dincer, 2020]) and non-renewable resources (e.g., oil and gas [Bentley, 2002]). There is also growing interest in harvesting minerals from the seafloor [Teague et al., 2018], but our understanding of the sustainability and potential impacts of deep-sea mining on marine ecosystems and these global processes remain limited [Van Dover, 2011; Miller et al., 2018]. While the total marine biomass significantly outweighs that of terrestrial organisms [Bar-On et al., 2018], our understanding of marine life lags considerably behind our understanding of terrestrial organisms [Mora et al., 2011]. The growing pressures for resource extraction make the need for understanding human impacts on marine environments even more pressing.

Despite the global, interconnected nature of these processes, exploration and study have been concentrated in only a few regions. Images of the deep-sea [Katija et al., 2022] and measurements of basic parameters such as salinity, temperature, and depth

(CTD) provide a substantial amount of information towards understanding environmental conditions, but the means of collecting this data are not available to many researchers around the world [Commission et al., 2020; Bell et al., 2022]. Physical seafloor samples with complementary *in-situ* measurements also play a key role in oceanographic research [Huguen et al., 2009], but similarly, there exist large disparities in access to deep submergence assets such as ROVs, AUVs, benthic landers, drifters, towsleds, and HOVs between different regions of the world. Since these technologies are more accessible to scientists in industrialized nations, there are significant knowledge gaps that result from the biased distribution of regions which are studied. The lack of affordable, efficient, and equitable approaches to study the deep-sea limits our understanding of global ocean processes [Bell et al., 2022].

In response to these challenges, there are ongoing efforts to prioritize collaborative research methods which promote inclusion, accessibility, and equity within the field of oceanography [Bell et al., 2022; Meyer-Gutbrod et al., 2023]. These efforts take on various forms, such as conducting collaborative design study on technological needs for deep-sea exploration [Bell et al., 2022], creating databases to make large amounts of oceanographic data widely available [Katija et al., 2022; Isern and Clark, 2003], and utilizing AI tools to help process large datasets or camera imagery [Ditria et al., 2022]. Furthermore, publicly accessible video streams enable people to observe deep-sea research in real-time [Raineault, 2019].

In recent years, there has been a growing interest in developing low-cost methods for studying the ocean as a means of increasing accessibility to oceanographic research. For shallow-water study, open-sourced camera and sensor systems for monitoring have been developed using low-cost, commercially available components [Butler and Pagniello, 2022]. In deeper regions, developments in towed underwater camera systems [Trobbiani et al., 2018], deep-sea camera systems [Dominguez-Carrió et al., 2021], and miniaturized cameras for landers [Giddens et al., 2021] increase portability and ease of operations while decreasing costs. While these methods suffice for observation, they are limited in their ability to retrieve physical samples or take measurements with sensors that require precise positioning or dexterity to operate. Relatively lower-cost

methods of seafloor sampling include trawls and grabs, but these methods are more intrusive and less precise than sampling with more sophisticated technology such as ROVs and HOVs [Dominguez-Carrió et al., 2021]. There is a need for sampling tools that can generate new deep-sea scientific data at a reasonable cost to make exploration more accessible [Montagna et al., 2017].

Prior work with telepresence has improved the accessibility of shipboard operations by making data and video available to shore-side users in real-time and supporting discussion among onshore and offshore collaborators [Martinez and Keener-Chavis, 2006]. Increasing the capabilities of shore-side collaborators beyond data monitoring and discussion holds potential for further improving accessibility to deep-sea research. As discussed in Chapter 3, the SHARC framework enabled remote scientists without prior manipulator operations experience to successfully collect seafloor samples and *in-situ* measurements, which demonstrates a step towards more active involvement by shore-side users during shipboard operations. For a more comprehensive evaluation of SHARC against the conventional topside controller interface pilots use for seafloor sampling beyond this field demonstration, we conducted a user study, which is discussed in detail in this chapter.

4.2 Experimental Validation: User Study

We conducted a user study to quantitatively compare users' performance with SHARC against a conventional topside control interface for underwater manipulators. This study recorded participants' performance on key performance benchmarks (i.e. precision, accuracy, task completion rate, and time) while completing representative manipulation tasks with each of the interfaces. The objectives of this study are summarized as follows:

- Compare participants' precision, accuracy, task completion rate, and time with each interface
- Evaluate the effect of prior manipulator operations experience on performance with each interface

- Evaluate comparative performance between the interfaces in low-bandwidth conditions
- Examine the learning curve for each interface for both novice and expert users

4.2.1 Participants

This study involved four different test groups, consisting of trained ROV pilots and novices using the topside controller and SHARC-VR interfaces. Some participants used both the VR and topside controller interfaces while others used only one depending on their availability. All participants were employees at the Woods Hole Oceanographic Institution (WHOI) who were recruited over email and selected on a first-come first-serve basis. Table 4.1 provides the number of participants within each group.

Test group	# of participants
ROV pilots using the topside controller	5
ROV pilots using SHARC-VR	6
ROV pilots TOTAL	6
Novices using the topside controller	9
Novices using SHARC-VR	8
Novices TOTAL	17

Table 4.1: Number of participants in each of the four user study test groups, which consisted of ROV pilots and novices using the topside controller and SHARC-VR interfaces. Some participants tested both interfaces, and thus are in two different test groups.

4.2.2 Experimental Setup & Testing Procedure

Participants from these tests groups completed representative manipulation tasks in timed trials using the SHARC-VR (Figure 2-4) and conventional topside controller (Figure 4-1) interfaces. During the study, participants operated a laboratory-based (in-air) testbed (Figure 4-2) with the same manipulator model deployed on the HROV Nereid Under Ice (NUI) vehicle [Bowen et al., 2014] in the field demonstrations described in Section 3.3. The testbed consists of a seven degree-of-freedom hydraulic



Figure 4-1: Photo of the conventional topside controller used to control the hydraulic manipulator arm during user testing

manipulator (Kraft TeleRobotics; Overland Park, KS) with a sandbox placed approximately within the reachable workspace of the arm when it is mounted onboard the NUI vehicle. The setup includes cameras and a tool basket containing a push core with their positions consistent with their placement onboard NUI. As a proxy for an underwater imaging system (e.g., stereo camera [Ishibashi, 2009], laser scanner [Palomer et al., 2018], or imaging sonar [Guerneve and Petillot, 2015]), an Xbox One Kinect (Microsoft; Redmond, WA) was used to generate the 3D workspace reconstruction during user studies with the in-air testbed. This sensor was installed in a location relative to the manipulator that closely approximates the position of the stereo cameras located onboard the NUI vehicle.

The manipulator testbed was located in an area separate from the participants in order to maximize safety, as illustrated in Figure 4-3. When learning how to use the topside controller, participants stood in the “training area” outside of the arm’s workspace, but maintained a direct line-of-sight to the physical arm. During testing, participants operated the arm from a separate room using either the SHARC-VR or topside controller interfaces while an evaluator monitored the physical arm from the training area. When testing the SHARC-VR interface, the evaluator was able to

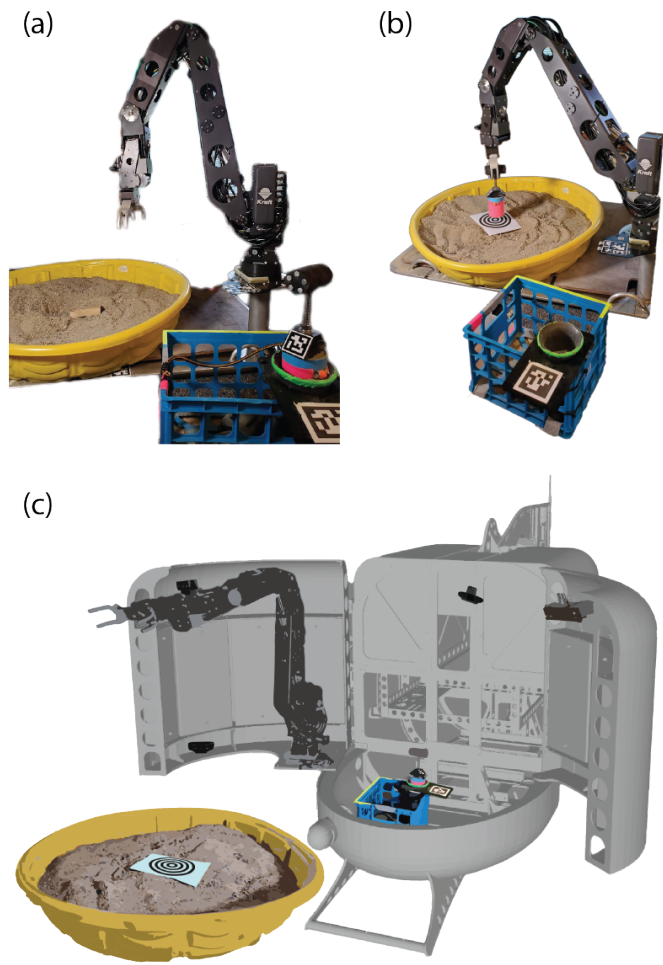


Figure 4-2: The in-air testbed used for user study consists of a hydraulic manipulator equipped with a basket for tools and samples, and can be configured to simulate a sample retrieval task (a) or a push-core sampling task (b). (c) The manipulator, camera, tool basket, and workspace position on the testbed (colored) closely resemble those on the physical vehicle (displayed in monochrome, for reference)

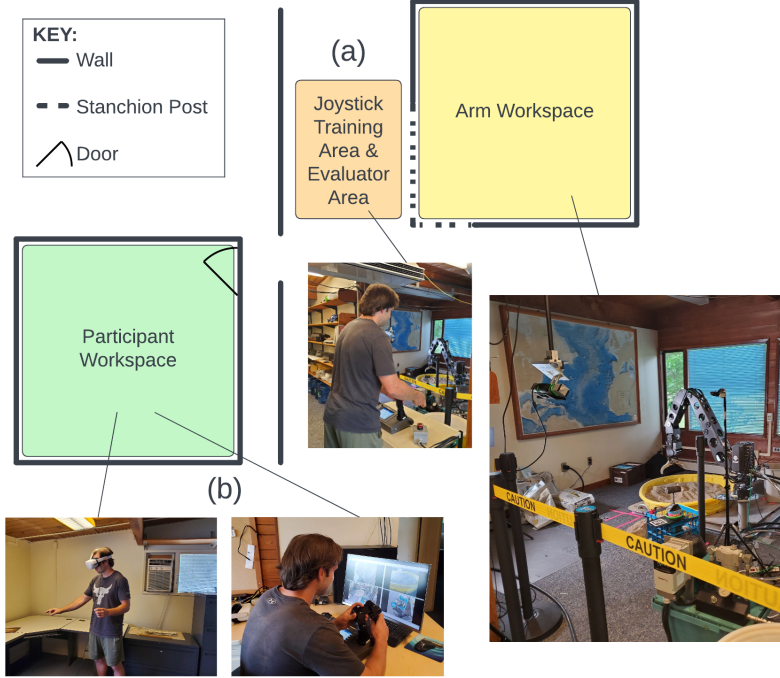


Figure 4-3: Illustration of the testing layout for the comparative user study. Participants gained familiarity with the conventional topside controller in the “training area” with direct line-of-sight to the physical arm (a), but operated the controller and the SHARC-VR interface in a separate room during testing (b).

observe the participant’s headset view and the automated system’s planned arm trajectories. The evaluator stopped the trial if the participant crashed the manipulator, caused an irrecoverable state (e.g. dropped a tool outside workspace), or exceeded 10 minutes in their attempt to complete the task.

Participants from the novice user group completed a 15 minute tutorial before completing timed trials with the SHARC-VR interface, and completed a 6 minute tutorial followed by 25 minutes of practice before testing with the topside controller interface. Pilots tested on the SHARC-VR interface were given the same SHARC-VR tutorial, while pilots tested on the topside controller were given a 10-minute “warm-up” period instead of a tutorial.

Participants completed two tasks with each of the interfaces, which involved (1) retrieving a wooden block from a sandbox and placing it in a basket, which is mechanically similar to collecting a rock sample in a natural, unstructured environment, and (2) pressing a push core through a paper target “bullseye,” which is analogous

to taking a push core sample in a heterogeneous microbial mat. These tasks are representative of a lower and higher precision task, respectively.

To simulate the effects of communication bandwidth constraints on different orders of magnitude, participants repeated these tasks with a variety of different visual update rates of the workspace environment (referred to as frames-per-second or FPS). The block pick-up task was tested at 10, 1.5, 0.5, 0.2, and 0.1 FPS. The push core task was tested at 10, 0.5, and 0.1 FPS. To measure sampling precision and accuracy, the distance between the center of the punch in the sheet of paper and the center of the printed “bullseye” was recorded.

4.2.3 Results

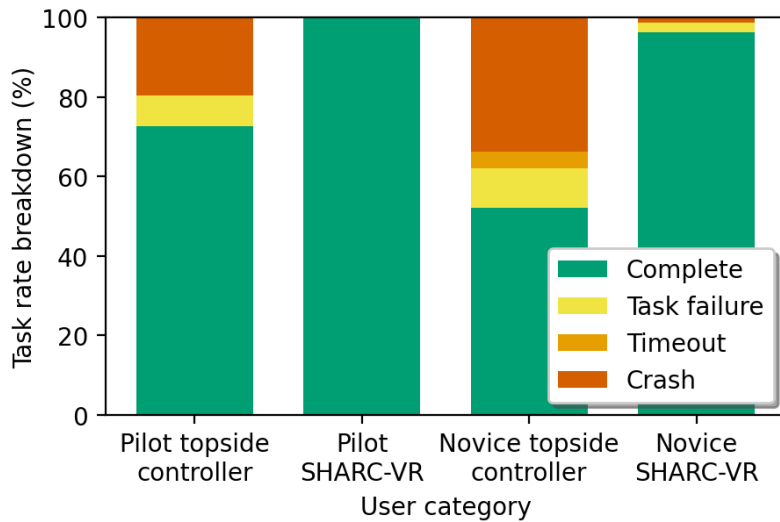
Based on the outcome, each timed trial was labeled as “complete” (i.e. the participant successfully collected the sample), “failed” (i.e. the participant caused an unrecoverable state, such as dropping the block or tool out of reach), “timed out” (i.e. the participant took too long to complete the task), or “crashed” (i.e. the evaluator stopped the arm to prevent collision damage). The frequency of these outcomes for each test group is illustrated in Figure 4-4a. The *Task Completion Rates* at each FPS, defined as

$$R_{\text{fps}} = \frac{\# \text{ of “complete” trials}}{\# \text{ of trials}}$$

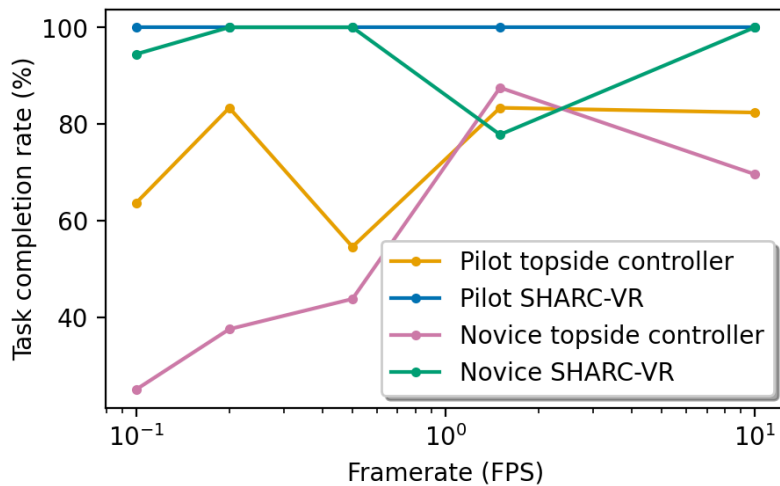
are presented in Figure 4-4b.

As shown in Figure 4-4, SHARC significantly increased *Task Completion Rates* among pilots and novices (Figure 4-4a) across nearly all camera framerates (Figure 4-4b). This increase is most pronounced at low framerates; at 0.1 FPS, the completion rate among pilots and novices were, respectively, 57% and 278% higher with SHARC than with the conventional topside controller. On average, pilots exhibited a higher completion rate than novices with both interfaces.

Figures 4-5a and 4-5b display the recorded *Task Completion Times* $T_{i,\text{FPS}}$ for each block-pickup and push core trial i across framerates. Figure 4-5c shows the *Expected Task Times* $\mathbb{E}[T_{\text{FPS}}]$ across framerates, which is computed as the average recorded



(a)



(b)

Figure 4-4: (a) Frequency of trial outcomes per test group. (b) *Task Completion Rate* (R_{FPS}) among test groups, expressed across framerates. Across most framerates, both pilots and novices had a higher *Task Completion Rate* with SHARC-VR than with the topside controller.

Task Completion Time \bar{T}_{FPS} divided by the *Task Completion Rate* R_{FPS} as follows:

$$\bar{T}_{\text{FPS}} = \frac{1}{n_{\text{FPS}}} \sum_{i=1}^{n_{\text{FPS}}} T_{i,\text{FPS}}$$

$$\mathbb{E}[T_{\text{FPS}}] = \frac{\bar{T}_{\text{FPS}}}{R_{\text{FPS}}}$$

Mathematically, this considers each trial as an independent event with a probability R_{FPS} of success, which implicitly assumes participants can retry failed tasks until successful. In Figure 4-5, a power curve is fit to the topside controller data because participants' times increased exponentially with decreasing framerates. For SHARC-VR, a linear trend is fit to the data because the times remained relatively constant across framerates.

At 10 FPS, novices had a significantly lower expected time with SHARC-VR than with the topside controller (95% CI), but there was no statistically significant difference (95% CI) between pilots' expected time with both interfaces. At 0.5 FPS or less, the expected time for both pilots and novices was faster with SHARC-VR than with the topside controller, and this difference increased as the framerate decreased. At 0.1 FPS, the expected time was 2X faster for pilots with SHARC-VR than with the topside controller and 7.6X faster for novices. Across all framerates, there is no statistically significant difference (95% CI) between the expected time for pilots and novices when using SHARC-VR, and the variance in times with SHARC-VR is less than that of the topside controller for both groups.

To more closely examine the learning rate among pilots and novices during testing, we compute the *Expected Task Time* of the block pick-up task for each group based on trial number instead of framerate (defined as $\mathbb{E}[T_{\text{trial}}]$) and observe how it changes based on the order of the trials. This analysis is presented in Figure 4-6. The expected time with SHARC-VR appears to be linear and independent of framerate, with a slope of -9.7 s/trial for pilots and -6.6 s/trial for novices. This is not the case with the topside controller, whose expected time appears to be dependent on framerate rather than trial number. The differences between the expected times of

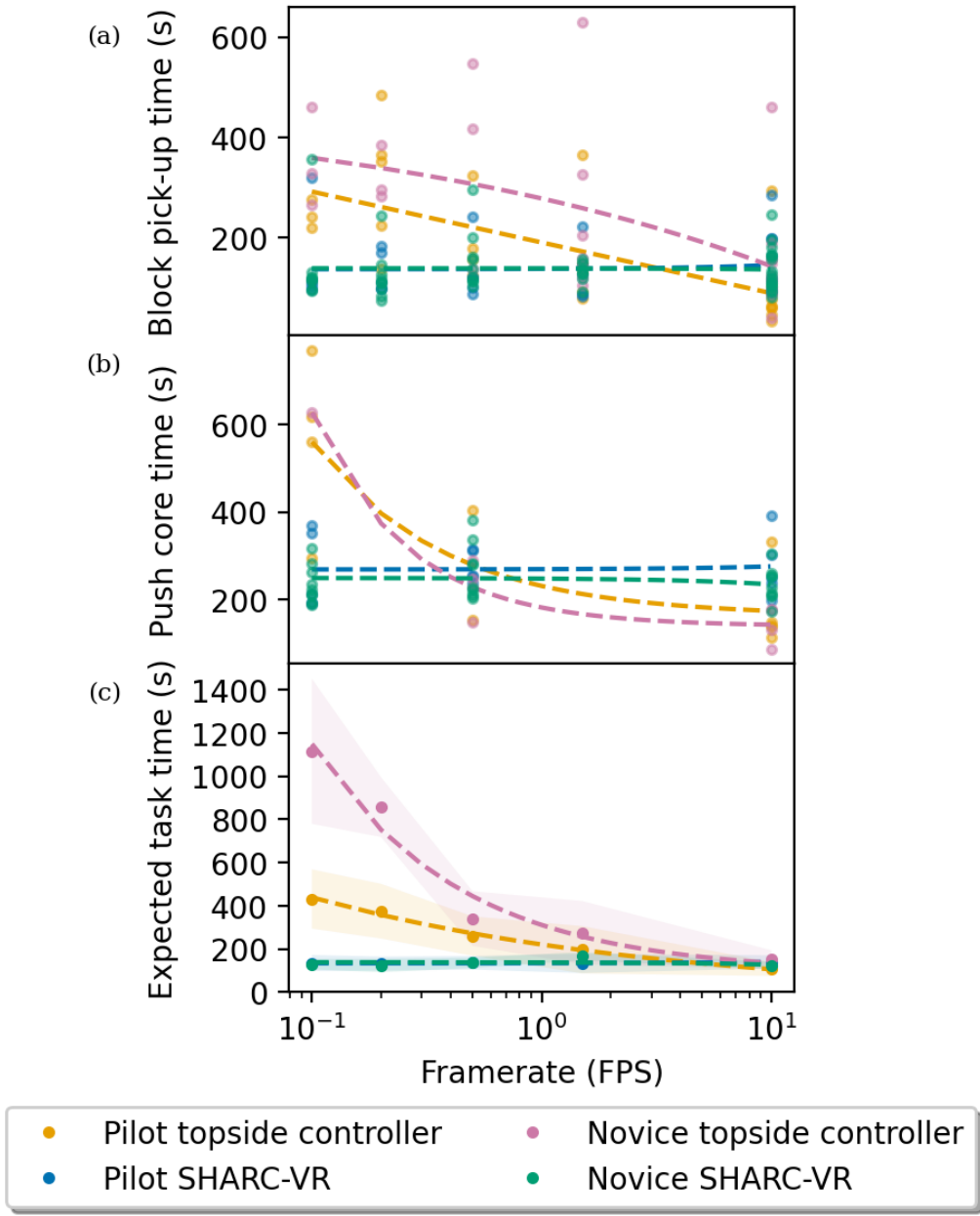


Figure 4-5: Plots of *Task Completion Times* $T_{i,\text{FPS}}$ for the block pick-up (a) and push core (b) tasks as well as the *Expected Task Times* $\mathbb{E}[T_{\text{FPS}}]$ (c) across framerate. A power and linear trend are fitted to the topside controller and SHARC-VR data, respectively. The 2σ distribution of points at each framerate is shaded in (c). At decreased framerates, pilots and novices complete both the block pick-up and push core tasks quicker with SHARC-VR than with the topside controller. This difference is more pronounced among the *Expected Task Times*, which factors in the *Task Completion Rate*

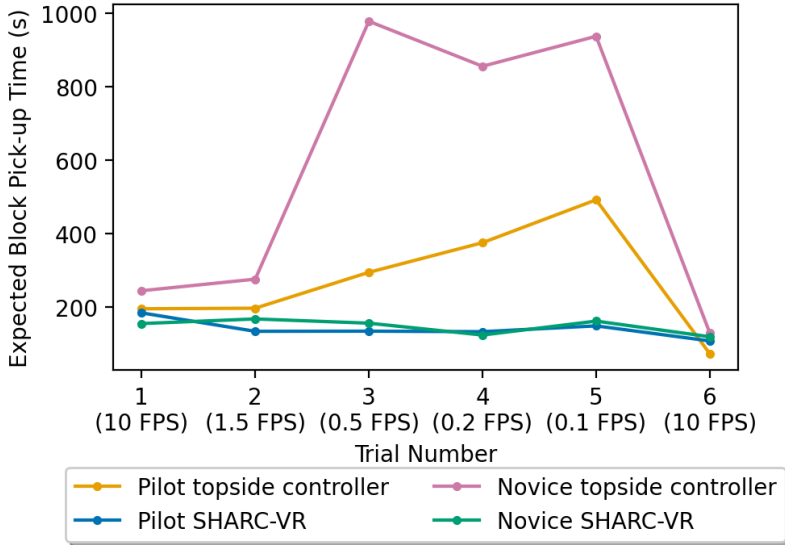


Figure 4-6: *Expected Task Times* $\text{E}[T_{\text{trial}}]$ for the block pick-up task plotted by trial number. Initial and final trials are conducted at 10 FPS to control for framerate. SHARC-VR times exhibit a slight negative correlation with trial number independent of framerate, while topside controller times appear to be framerate dependent.

the first block pick-up trial $\text{E}[T_1]$ and the last trial $\text{E}[T_6]$ are recorded in Table 4.2.

During the initial trial at 10 FPS, novices using SHARC-VR exhibited the fastest *Expected Task Time* across all test groups. However, during the final trial at 10 FPS (~30 min into testing), pilots using the topside controller were the fastest, which is unsurprising given their familiarity with the conventional control interface. For both operator groups, the differences between the first and last trials were smaller when using SHARC-VR than when using the topside controller.

	Initial Time $\text{E}[T_1]$	Final Time $\text{E}[T_6]$	Absolute Improvement $\text{E}[T_6] - \text{E}[T_1]$	Relative Improvement $\frac{\text{E}[T_6] - \text{E}[T_1]}{\text{E}[T_1]}$
Pilot topside controller	195	72.7	122.3	63%
Pilot SHARC-VR	183.8	107.4	76.4	42%
Novice topside controller	244.2	129.3	114.9	47%
Novice SHARC-VR	154.7	118.8	35.9	23%

Table 4.2: Absolute and relative improvements in *Expected Task Time* $\text{E}[T_{\text{trial}}]$ for each test group between the initial and final block-pickup trials. The absolute and relative improvements were smaller with the SHARC-VR interface than with the topside controller for both pilots and novices.

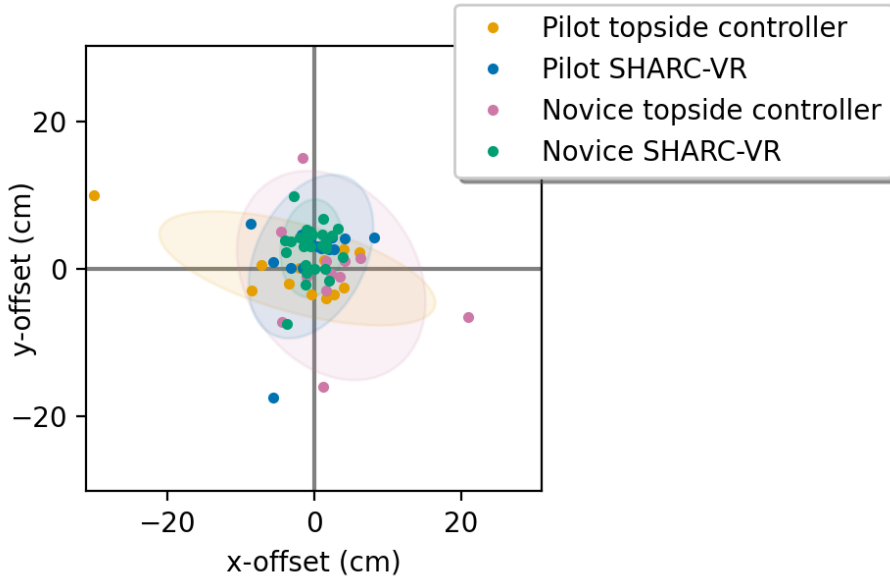


Figure 4-7: Map of push core placement locations by test group relative to the target center. Confidence ellipses (2σ) are shown for each group. For both pilots and novices, push core locations achieved using the SHARC-VR formed a tighter confidence ellipse than those with the topside controller.

To quantify participants' accuracy and precision with the two interfaces, the push core locations are recorded relative to the center of a target. Figure 4-7 visualizes this data, while Table 4.3 presents the average accuracy and precision for each group.

As shown in Table 4.3, pilots using SHARC-VR were the most accurate across all groups, and the SHARC-VR interface increased precision for both pilots and novices. Novices using SHARC-VR had the best precision, but the worst accuracy of all test groups. On average, using the SHARC-VR interface instead of the topside controller

	Accuracy (cm)	Precision (cm)
Pilot topside controller	2.3	7.0
Pilot SHARC-VR	1.7	4.9
Novice topside controller	2.5	6.8
Novice SHARC-VR	2.8	3.3

Table 4.3: Ensemble accuracy and precision of push core placement per test group. On average, users demonstrated greater precision with SHARC-VR than with the topside controller. Pilots using SHARC-VR exhibited the highest accuracy across all test groups.

decreased the variance between participants' placement position by $\sim 30\%$ for pilots and $\sim 52\%$ for novices. Pilots and novices using the topside controller had comparable accuracy and precision.

4.3 Discussion

In contrast to conventional interfaces, SHARC enables users to operate with performance benchmarks (i.e., precision, accuracy, task time, and task completion rate) comparable to that of trained pilots regardless of their prior experience, even when faced with bandwidth limitations. For both pilots and novices, *Task Completion Rates* R_{fps} when using SHARC-VR were generally higher than those obtained using the topside controller across tested framerates (Figure 4-4). These results suggest that SHARC increases the probability of successful task completion in operational settings, thereby minimizing time-consuming failures that can damage the vehicle platform or sensitive environments. Catastrophic failures that compromise platform survivability can jeopardize entire science campaigns, and thus SHARC may increase operations tempo while minimizing risk. At framerates below 10 FPS, pilots and novices using SHARC-VR had a faster *Expected Task Time* $\mathbb{E}[T_{FPS}]$ than pilots using the conventional topside controller (Figure 4-5c). Furthermore, as the framerate decreases, the topside controller's *Expected Task Time* increases exponentially from 107 s at 10 FPS to 432 s at 0.1 FPS for pilots, and 151 s to 1115 s for novices. In operational settings, these observed differences in *Expected Task Time* would likely be magnified since additional time would be needed to recover from failures, which are more likely to occur with the topside controller than with SHARC-VR.

Surprisingly, the *Expected Task Times* with SHARC-VR exhibits a decreasing trend as the trials progressed, which appear to be independent of the framerate. Results indicate an average slope of -9.7 s/trial and -6.6 s/trial for pilot and novice groups, respectively, when using SHARC-VR to complete the block pick-up task (Figure 4-6). It would be reasonable to expect the decrease in camera framerates between trials 1 through 5 to cause the expected task time to increase with each

subsequent trial, as it does when participants use the topside controller; however, the observed trend with the SHARC-VR interface suggests otherwise. With SHARC-VR, the negative slope in time across trials suggests that any speed decrease caused by operating the manipulator at lower framerates may have been offset by the efficiency increase due to participant learning as the tests progressed.

As shown in Table 4.2, the differences between the *Expected Task Times* for the initial and final block pick-up trials at 10 FPS were greater when using the topside controller than when using SHARC-VR for both pilots and novices. This implies that the topside controller has an inherently steeper learning curve than SHARC-VR, and that operator performance is highly dependent on familiarity with the topside configuration (e.g., camera views, workspace layout, and controller settings). It is notable that one pilot failed the first block pick-up trial with the topside controller but succeeded in the final one, demonstrating that even trained pilots risk failure when not fully familiar with a conventional controller’s configuration settings.

Both novices and pilots using SHARC-VR exhibited small but consistent speed improvements with each successive trial regardless of framerate, indicating that the *Expected Task Time* is more strongly correlated with learning than with the tested framerates. In contrast, the *Expected Task Times* for the topside controller interface increased exponentially as framerate decreased, with this effect dominating any improvement achieved through learning. Future work could evaluate whether these trends hold as the framerate decreases by additional orders of magnitude, or across extended numbers of trials.

In our experiments, VR users averaged \sim 133 s to complete a block pick-up at 0.1 FPS, which translates to only 13 frames of data for the entire task. Theoretically, with a static scene, only three frames of data should be necessary: one to determine the target position in the workplace, a second to confirm the target has been grasped, and a third to confirm that the target has been retrieved successfully. Future work could relax this static scene assumption by implementing a process to identify changes to the scene and adapt the reconstruction or manipulation plan as necessary.

By reducing the required bandwidth needed for operation by two orders-of-magnitude

	Acoustic	Optical	Light Fiber	Conventional Tether
Bandwidth	30-100 kbit/s	1-10 Mbit/s	Multiple Gbit/s	Multiple Gbit/s
FPS	0.03-0.125	1.25-12.5	30+*	30+*
Range	several km	<150 m	>20 km horizontal or vertical	<1 km horizontal, 6 km vertical
Expected Task Time				
>Pilot Topside Controller	7:11	1:47-3:16	1:47	1:47
>Pilot SHARC-VR	2:15	2:13-2:20	2:20	2:20
>Novice Topside Controller	18:35	2:31-4:36	2:31	2:31
>Novice SHARC-VR	2:10	2:04-2:47	2:04	2:04

Table 4.4: Estimated frame update rates with various underwater communication methods, computed based on bandwidth limitations reported by Bowen et al. [2013]. Framerate estimates assume standard-definition (SD) resolution (640 x 480 px) from 2 camera feeds. The listed times (min:sec format) are based on the *Expected Task Time* from the nearest recorded framerate illustrated in Figure 4-5c.

(from 10 FPS to 0.1 FPS), SHARC shows the potential to enable tether-less manipulation operations. Figure 4-8 illustrates the framerates tested during the user study in context of bandwidth limitations imposed by current through-water communication methods as described in Table 4.4. Existing commercial through-water optical modems can transmit up to 10 Mb/s [Alexander et al., 2021], which could theoretically support SHARC-VR at more than 10 FPS. Future optimization may enable the use of lower bandwidth acoustic modems that can transmit at 5.3 kb/s [Singh et al., 2009], which would theoretically support an update rate of 0.02 FPS. Supporting this update rate at this bandwidth necessitates an update packet size of 265 kb or less, which should be sufficient for robotic manipulation with framerate-limited feedback [Billings et al., 2022b]. Under these bandwidth constraints, a standard cloud-based shore server using a gigabit uplink could support more than a million observers, any of whom can be designated as an operator.

SHARC’s ability to engage remote users can significantly decrease the barriers to access deep-ocean sampling and research. As the results from this user study indicate,

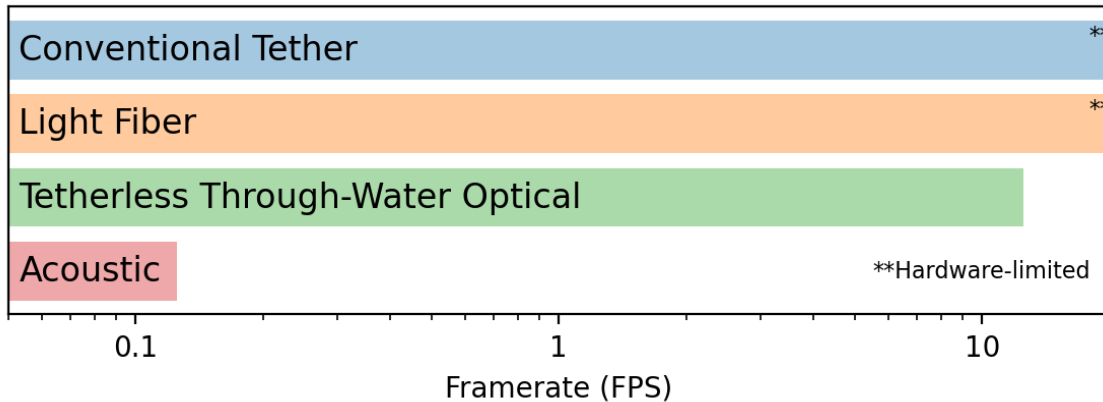


Figure 4-8: Visual illustration of the supported framerates for the underwater communication methods listed in Table 4.4. The maximum framerate with communications across the conventional tether or light fiber is limited by the camera’s hardware rather than the communication method.

SHARC’s lower learning curve enables novice users without prior piloting experience to achieve comparable performance to skilled pilots using the conventional interface with a 10 FPS update rate, and better performance in low-bandwidth conditions (<10 FPS). Enabling both skilled and novice users to safely operate manipulators in low-bandwidth conditions brings us closer to a future with tetherless intervention robots that don’t require support from a surface ship, which would significantly reduce the operational costs. By making deep-sea science more cost-effective, reducing the training and experience required for participation, and enabling shore-side participation by users with only a basic Internet connection and off-the-shelf consumer-grade hardware, SHARC demonstrates significant potential for democratizing access to deep-sea science.

Chapter 5

Discussion and Future Work

5.1 Contributions

This thesis presents the SHared Autonomy for Remote Collaboration (SHARC) framework, which aims to improve the capabilities of exploration robots in remote environments. As discussed in Chapter 2, SHARC adopts a distributed approach to allocate tasks between robots and human operators based on their respective strengths, and incorporates natural interfaces such as language and gestures to improve usability among novice users. By using shared autonomy and natural interfaces, SHARC promotes task parallelization and reduces the cognitive load on operators, which in turn should lead to increases in operational efficiency and robustness, particularly in bandwidth-limited conditions.

To evaluate SHARC’s functionality in operational settings, the framework was used during field trials as discussed in Chapter 3. During these trials, SHARC enabled a shore-side science team to conduct seafloor elemental analysis and physical sample collection with centimeter-level spatial precision. This demonstration provides compelling evidence of SHARC’s utility for conducting delicate operations in unstructured environments across bandwidth-limited communications, which holds relevance for improving operations in other sensitive domains where dexterity is required.

In Chapter 4, a controlled user study evaluated SHARC’s performance with regards to performance benchmarks such as precision, accuracy, and task completion

rates and times. Results demonstrated SHARC’s ability to enable users to achieve better performance benchmarks when completing representative manipulation tasks than skilled pilots using the conventional controller, particularly in the presence of bandwidth limitations. These results indicate that SHARC enables efficient human-collaborative manipulation in complex, unstructured environments, and can outperform conventional teleoperation in certain operational conditions. SHARC’s ability to support novice shore-side users without requiring additional bandwidth from the ship or specialized hardware has potential to further democratize access to deep sea operations.

5.2 Future work

5.2.1 Robust Perception in Turbid Conditions

By utilizing human perception for semantic-level scene understanding while delegating low-level control and 3D scene reconstruction to the automated system, SHARC enables users to achieve improved performance benchmarks in comparison to conventional controllers. However, existing methods for 3D scene reconstruction with optical imagery heavily rely on local feature matching [Beall et al., 2010], which leads to poor performance in areas lacking discernable landmarks. Turbid conditions, which may occur naturally or arise due to vehicle and manipulator movement, can also significantly hamper SHARC’s capabilities due to its reliance on optical cameras for perception.

With their longer operational wavelength, acoustic sensors are less affected by scattering caused by turbid conditions than optical cameras, which enable them to operate in zero-visibility conditions [Cong et al., 2021]. Attributes of acoustic returns (e.g., backscatter, intensity), also possess the ability to characterize material properties which may not be discernable by optical sensors [Cong et al., 2021; Duguid, 2020]. Prior work has fused optical and acoustic data for multimodal mapping [Hurtós et al., 2010; Ferreira et al., 2016]; however, adopting these methods for use onboard robotic

manipulators would require algorithmic or computational efficiency improvements to enable real-time operation. Incorporating acoustic sensing methods to augment SHARC’s existing optical perception system can vastly improve our intervention capabilities in remote, unstructured environments, and enable scientists to visualize material properties previously imperceptible by optical imaging systems.

5.2.2 Improved Control Methods

Additional improvements to SHARC’s control method could optimize tradeoffs between execution time, power requirements, and accuracy during manipulation. Currently, SHARC uses a standard PID controller to move each joint along a pre-computed manipulator trajectory. This controller is prone to acceleration-induced overshoot, which is currently mitigated by limiting the joint rotation rate. Even with these limits, our control method only achieved centimeter-level accuracy at best. Future work could use a model predictive controller [Varga et al., 2019] to enable faster actuation rates while minimizing this overshoot, and infer accuracy requirements based on the user’s actions to scale the planning and execution times accordingly. SHARC’s positioning accuracy could also be improved with the integration of a visual servoing-based controller, which has achieved millimeter-level accuracy with similar manipulators [Sivčev et al., 2018]. Augmenting the planner to optimize for trajectories that minimize power usage would also be valuable for vehicles that carry power onboard, such as the NUI vehicle used during our field demonstration.

5.2.3 Adapting to Dynamic Obstacles

SHARC’s current plan-then-execute approach implicitly assumes the environment is quasi-static, which can be problematic if a planned trajectory causes the arm to collide with dynamic obstacles that have moved since planning. Incorporating methods for local change detection [Rout et al., 2018] would enable SHARC to detect moving objects in the workspace that could pose a collision risk. Future work could also incorporate dynamic replanning methods [Zucker et al., 2007; Dai et al., 2021], which

would route the arm around newly detected obstacles in the workspace. These perception and planning improvements would enable SHARC to safely operate in dynamic environments, which would extend its capabilities and while increasing operational robustness.

5.2.4 Integration on Multi-Manipulator Systems

SHARC is platform independent and can be readily integrated onto other underwater vehicles equipped with at least one robotic manipulator, a workspace imaging sensor, and a means to communicate with operators. SHARC’s current implementation supports single-manipulator platforms, but future work could extend the framework to multi-manipulator systems [Li et al., 2015] distributed across one or more vehicles with more than one concurrent operator [Soroushpour and Setoodeh, 2005]. Currently, operations involving multiple vehicles or manipulator arms are completed sequentially, with only one vehicle or manipulator operating at any given time. These operations require pilots to maintain situational awareness of all of the assets involved in addition to their interactions with the natural unstructured environment, which imparts additional cognitive load on the pilot. In contrast to the sequential operations approach, coordinated manipulation could enable vehicles to manipulate objects too large or heavy for one manipulator to handle alone [Xian et al., 2017; Smith et al., 2012], complete tasks that require higher dexterity or redundant degrees-of-freedom [Smith et al., 2012], and operate more efficiently by parallelizing tasks. For a single operator, a dual manipulator setup can potentially reduce cognitive load since human operators are already accustomed to bimanual control [Smith et al., 2012].

5.3 Conclusion

Current methods for deep-ocean exploration require substantial resources, which presents multiple barriers to access for those who may lack the resources, time, or physical ability required for at-sea participation in oceanographic research. The SHARC framework presented in this thesis enables shore-side users to view real-time

data, participate in discussions, and control robotic manipulators using only an Internet connection and consumer-grade hardware, regardless of their prior piloting experience. SHARC’s ability to relax infrastructure requirements and engage with remote users provides a promising avenue for democratizing access to the deep-sea, and expanding scientific engagement to the broader audience of shore-side scientists, students, enthusiasts, and the general public.

Bibliography

- B. Alexander, S. Felix, and M. Igor. Practical applications of free-space optical underwater communication. In *2021 Fifth Underwater Communications and Networking Conference (UComms)*, pages 1–5. IEEE, 2021.
- M. Y. Alexandrin, A. V. Darin, I. A. Kalugin, E. A. Dolgova, A. M. Grachev, and O. N. Solomina. Annual sedimentary record from lake donguz-orun (central caucasus) constrained by high resolution sr-xrf analysis and its potential for climate reconstructions. *Frontiers in Earth Science*, 6:158, 2018.
- A. Allwood, B. Clark, D. Flannery, J. Hurowitz, L. Wade, T. Elam, M. Foote, and E. Knowles. Texture-specific elemental analysis of rocks and soils with pixl: The planetary instrument for x-ray lithochemistry on mars 2020. In *2015 IEEE Aerospace Conference*, pages 1–13. IEEE, 2015.
- A. C. Allwood, L. A. Wade, M. C. Foote, W. T. Elam, J. A. Hurowitz, S. Battel, D. E. Dawson, R. W. Denise, E. M. Ek, M. S. Gilbert, et al. Pixl: Planetary instrument for x-ray lithochemistry. *Space Science Reviews*, 216:1–132, 2020.
- B. J. Ayton. *Query-Driven Adaptive Sampling*. PhD thesis, Massachusetts Institute of Technology, 2022.
- K. K. Babarahmati, C. Tiseo, Q. Rouxel, Z. Li, and M. Mistry. Robust high-transparency haptic exploration for dexterous telemanipulation. In *2021 IEEE International Conference on Robotics and Automation (ICRA)*, pages 10146–10152. IEEE, 2021.
- R. D. Ballard and W. Hively. *The eternal darkness: a personal history of deep-sea exploration*, volume 50. Princeton University Press, 2017.
- Y. M. Bar-On, R. Phillips, and R. Milo. The biomass distribution on earth. *Proceedings of the National Academy of Sciences*, 115(25):6506–6511, 2018.
- C. Beall, B. J. Lawrence, V. Ila, and F. Dellaert. 3d reconstruction of underwater structures. In *2010 IEEE/RSJ International Conference on Intelligent Robots and Systems*, pages 4418–4423. IEEE, 2010.
- K. L. Bell, J. S. Chow, A. Hope, M. C. Quinzin, K. A. Cantner, D. J. Amon, J. E. Cramp, R. D. Rotjan, L. Kamalu, A. de Vos, et al. Low-cost, deep-sea imaging

- and analysis tools for deep-sea exploration: a collaborative design study. *Frontiers in Marine Science*, 9:873700, 2022.
- J. G. Bellingham and K. Rajan. Robotics in remote and hostile environments. *science*, 318(5853):1098–1102, 2007.
- R. W. Bentley. Global oil & gas depletion: an overview. *Energy policy*, 30(3):189–205, 2002.
- M. G. Bertolini, A. Castelvetri, A. Chiozzi, L. Colombo, G. Curti, P. Grattagliano, F. Maccari, A. Pinelli, M. Piunti, and E. M. R. Santosa. Phase-a design of ice cream: a cost-effective mars sample return mission. 2021.
- S. Bhaskaran, J. E. Riedel, and S. P. Synnott. Autonomous optical navigation for interplanetary missions. In *Space Sciencecraft Control and Tracking in the New Millennium*, volume 2810, pages 32–43. SPIE, 1996.
- D. R. Billings, K. E. Schaefer, J. Y. Chen, and P. A. Hancock. Human-robot interaction: developing trust in robots. In *Proceedings of the seventh annual ACM/IEEE international conference on Human-Robot Interaction*, pages 109–110, 2012.
- G. Billings, R. Camilli, and M. Johnson-Roberson. Hybrid visual slam for underwater vehicle manipulator systems. *IEEE Robotics and Automation Letters*, 7(3):6798–6805, 2022a.
- G. Billings, M. Walter, O. Pizarro, M. Johnson-Roberson, and R. Camilli. Towards automated sample collection and return in extreme underwater environments. *Field Robotics*, 2:1351–1385, 2022b.
- A. Birk, T. Doernbach, C. Mueller, T. Łuczynski, A. G. Chavez, D. Koehntopp, A. Kupcsik, S. Calinon, A. K. Tanwani, G. Antonelli, et al. Dexterous underwater manipulation from onshore locations: Streamlining efficiencies for remotely operated underwater vehicles. *IEEE Robotics & Automation Magazine*, 25(4):24–33, 2018.
- A. D. Bowen, D. R. Yoerger, C. Taylor, R. McCabe, J. Howland, D. Gomez-Ibanez, J. C. Kinsey, M. Heintz, G. McDonald, D. B. Peters, et al. The nereus hybrid underwater robotic vehicle for global ocean science operations to 11,000 m depth. In *OCEANS 2008*, pages 1–10. IEEE, 2008.
- A. D. Bowen, M. V. Jakuba, N. E. Farr, J. Ware, C. Taylor, D. Gomez-Ibanez, C. R. Machado, and C. Pontbriand. An un-tethered rov for routine access and intervention in the deep sea. In *2013 oceans-san diego*, pages 1–7. IEEE, 2013.
- A. D. Bowen, D. R. Yoerger, C. C. German, J. C. Kinsey, M. V. Jakuba, D. Gomez-Ibanez, C. L. Taylor, C. Machado, J. C. Howland, C. L. Kaiser, et al. Design of nereid-ui: a remotely operated underwater vehicle for oceanographic access under ice. In *2014 Oceans-St. John's*, pages 1–6. IEEE, 2014.

- J. Breen, P. de Souza, G. Timms, J. McCulloch, and R. Ollington. Analysis of heavy metals in marine sediment using a portable x-ray fluorescence spectrometer onboard an autonomous underwater vehicle. In *2012 Oceans- Yeosu*, pages 1–5. IEEE, 2012.
- J. L. Bresina, A. K. Jónsson, P. H. Morris, and K. Rajan. Mixed-initiative planning in mapgen: Capabilities and shortcomings. In *Workshop on Mixed-Initiative Planning and Scheduling*, 2005.
- S. Bünz, E. Ramirez-Llodra, C. German, B. Ferre, F. Sert, D. Kalenichenko, E. Reeves, K. Hand, H. Dahle, T. Kutti, et al. Rv kronprins håkon (cruise no. 2019708) longyearbyen–longyearbyen 19.09.–16.10. 2019. 2020.
- J. Butler and C. Pagniello. Emerging, low-cost ocean observing technologies to democratize access to the ocean. *Oceanography*, 34:94–95, 2022.
- R. Camilli. Self-contained xrf for deep-sea operation. unpublished, 2019.
- R. Camilli, B. Bingham, M. Jakuba, H. Singh, and J. Whelan. Integrating in-situ chemical sampling with auv control systems. In *Oceans' 04 MTS/IEEE Techno-Ocean'04 (IEEE Cat. No. 04CH37600)*, volume 1, pages 101–109. IEEE, 2004.
- A. Ceballos, S. Bensalem, A. Cesta, L. De Silva, S. Fratini, F. Ingrand, J. Ocon, A. Orlandini, F. Py, K. Rajan, et al. A goal-oriented autonomous controller for space exploration. *ASTRA*, 11, 2011.
- F. Chai, K. S. Johnson, H. Claustre, X. Xing, Y. Wang, E. Boss, S. Riser, K. Fennel, O. Schofield, and A. Sutton. Monitoring ocean biogeochemistry with autonomous platforms. *Nature Reviews Earth & Environment*, 1(6):315–326, 2020.
- S. Chitta, I. Sucan, and S. Cousins. Moveit![ros topics]. *IEEE Robotics & Automation Magazine*, 19(1):18–19, 2012.
- P. Cieslak, P. Ridao, and M. Giergel. Autonomous underwater panel operation by girona500 uvms: A practical approach to autonomous underwater manipulation. In *2015 IEEE International conference on robotics and automation (ICRA)*, pages 529–536. IEEE, 2015.
- D. Comelli, M. D'orazio, L. Folco, M. El-Halwagy, T. Frizzi, R. Alberti, V. Capogrossi, A. Elnaggar, H. Hassan, A. Nevin, et al. The meteoritic origin of tutankhamun's iron dagger blade. *Meteoritics & Planetary Science*, 51(7):1301–1309, 2016.
- I. O. Commission et al. *Global Ocean Science Report: Charting Capacity for Ocean Sustainability*, volume 2020. UNESCO Publishing, 2020.
- Y. Cong, C. Gu, T. Zhang, and Y. Gao. Underwater robot sensing technology: A survey. *Fundamental Research*, 1(3):337–345, 2021.

- J. B. Corliss, J. Dymond, L. I. Gordon, J. M. Edmond, R. P. von Herzen, R. D. Ballard, K. Green, D. Williams, A. Bainbridge, K. Crane, et al. Submarine thermal springs on the galapagos rift. *Science*, 203(4385):1073–1083, 1979.
- E. Craven, M. Winters, A. L. Smith, E. Lalime, R. Mancinelli, B. Shirey, W. Schubert, A. Schuerger, M. Burgin, E. P. Seto, et al. Biological safety in the context of backward planetary protection and mars sample return: conclusions from the sterilization working group. *International Journal of Astrobiology*, 20(1):1–28, 2021.
- T. Crees, C. Kaminski, J. Ferguson, J. M. Laframboise, A. Forrest, J. Williams, E. MacNeil, D. Hopkin, and R. Pederson. Unclos under ice survey-an historic auv deployment in the canadian high arctic. In *OCEANS 2010 MTS/IEEE SEATTLE*, pages 1–8. IEEE, 2010.
- T. B. Curtin, J. G. Bellingham, J. Catipovic, and D. Webb. Autonomous oceanographic sampling networks. *Oceanography*, 6(3):86–94, 1993.
- S. Dai, A. Hofmann, and B. Williams. Fast-reactive probabilistic motion planning for high-dimensional robots. *SN Computer Science*, 2:1–39, 2021.
- E. M. Ditria, C. A. Buelow, M. Gonzalez-Rivero, and R. M. Connolly. Artificial intelligence and automated monitoring for assisting conservation of marine ecosystems: A perspective. *Frontiers in Marine Science*, 9:918104, 2022.
- C. Dominguez-Carrió, J. Fontes, and T. Morato. A cost-effective video system for a rapid appraisal of deep-sea benthic habitats: The azor drift-cam. *Methods in Ecology and Evolution*, 12(8):1379–1388, 2021.
- Z. Duguid. *Towards basin-scale in-situ characterization of sea-ice using an Autonomous Underwater Glider*. PhD thesis, Massachusetts Institute of Technology, 2020.
- Z. Duguid and R. Camilli. Improving resource management for unattended observation of the marginal ice zone using autonomous underwater gliders. *Frontiers in Robotics and AI*, 7:579256, 2021.
- K. Ebadi, K. Coble, D. Kogan, D. Atha, R. Schwartz, C. Padgett, and J. Vander Hook. Toward autonomous localization of planetary robotic explorers by relying on semantic mapping. In *2022 IEEE Aerospace Conference (AERO)*, pages 1–10. IEEE, 2022.
- A. Elor, T. Thang, B. P. Hughes, A. Crosby, A. Phung, E. Gonzalez, K. Katija, S. H. Haddock, E. J. Martin, B. E. Erwin, et al. Catching jellies in immersive virtual reality: A comparative teleoperation study of rovs in underwater capture tasks. In *Proceedings of the 27th ACM Symposium on Virtual Reality Software and Technology*, pages 1–10, 2021.

- H. F. Morrison, A. Becker, T. Smith, and E. Gasperikova. Detection and classification of buried metallic objects. In *64th EAGE Conference and Exhibition-Workshops*, pages cp–139. EAGE Publications BV, 2002.
- F. Ferreira, D. Machado, G. Ferri, S. Dugelay, and J. Potter. Underwater optical and acoustic imaging: A time for fusion? a brief overview of the state-of-the-art. *OCEANS 2016 MTS/IEEE Monterey*, pages 1–6, 2016.
- P. H. Figueredo, R. Greeley, S. Neuer, L. Irwin, and D. Schulze-Makuch. Locating potential biosignatures on europa from surface geology observations. *Astrobiology*, 3(4):851–861, 2003.
- J. Gancet, D. Urbina, P. Letier, M. Ilzokvitz, P. Weiss, F. Gauch, G. Antonelli, G. Indiveri, G. Casalino, A. Birk, et al. Dexrov: Dexterous undersea inspection and maintenance in presence of communication latencies. *IFAC-PapersOnLine*, 48(2): 218–223, 2015.
- A. L. Gemmell, R. Barciela, J. D. Blower, K. Haines, Q. Harpham, K. Millard, M. Price, and A. Saulter. An ecoop web portal for visualising and comparing distributed coastal oceanography model and in situ data. *Ocean Science*, 7(4): 445–454, 2011.
- J. Giddens, A. Turchik, W. Goodell, M. Rodriguez, and D. Delaney. The national geographic society deep-sea camera system: A low-cost remote video survey instrument to advance biodiversity observation in the deep ocean. *Frontiers in Marine Science*, page 1157, 2021.
- M. A. Goodrich, D. R. Olsen, J. W. Crandall, and T. J. Palmer. Experiments in adjustable autonomy. In *Proceedings of IJCAI Workshop on autonomy, delegation and control: interacting with intelligent agents*, pages 1624–1629. Seattle, WA, 2001.
- S. M. Goza, R. O. Ambrose, M. A. Diftler, and I. M. Spain. Telepresence control of the nasa/darpa robonaut on a mobility platform. In *Proceedings of the SIGCHI conference on Human factors in computing systems*, pages 623–629, 2004.
- T. Guerneve and Y. Petillot. Underwater 3d reconstruction using blueview imaging sonar. In *OCEANS 2015-Genova*, pages 1–7. IEEE, 2015.
- A. Hahn, M. Bowen, P. Clift, D. Kulhanek, and M. Lyle. Testing the analytical performance of handheld xrf using marine sediments of iodp expedition 355. *Geological Magazine*, 157(6):956–960, 2020.
- K. P. Hand, C. F. Chyba, J. C. Priscu, R. W. Carlson, and K. H. Nealson. Astrobiology and the potential for life on europa. *Europa*, pages 589–629, 2009.

- J. Hegde, I. B. Utne, and I. Schjølberg. Applicability of current remotely operated vehicle standards and guidelines to autonomous subsea imr operations. In *International Conference on Offshore Mechanics and Arctic Engineering*, volume 56550, page V007T06A026. American Society of Mechanical Engineers, 2015.
- B. L. Henke, E. M. Gullikson, and J. C. Davis. X-ray interactions: photoabsorption, scattering, transmission, and reflection at $e = 50\text{-}30000 \text{ ev}$, $z = 1\text{-}92$. *Atomic Data and Nuclear Data Tables*, 54(2):181–342, July 1993. doi: 10.1006/adnd.1993.1013. URL https://henke.lbl.gov/optical_constants/.
- P. Hintjens. *ZeroMQ: messaging for many applications*. " O'Reilly Media, Inc.", 2013.
- M. Hložek, T. Trojek, B. Komoróczy, and R. Prokes. Enamel paint techniques in archaeology and their identification using xrf and micro-xrf. *Radiation Physics and Chemistry*, 137:243–247, 2017.
- B. Hołyńska, B. Ostachowicz, and D. Wgrzynek. Simple method of determination of copper, mercury and lead in potable water with preliminary pre-concentration by total reflection x-ray fluorescence spectrometry. *Spectrochimica Acta Part B: Atomic Spectroscopy*, 51(7):769–773, 1996.
- S. Hopko, J. Wang, and R. Mehta. Human factors considerations and metrics in shared space human-robot collaboration: a systematic review. *Frontiers in Robotics and AI*, 9:6, 2022.
- S. E. Houts, S. M. Rock, and R. McEwen. Aggressive terrain following for motion-constrained auvs. In *2012 IEEE/OES Autonomous Underwater Vehicles (AUV)*, pages 1–7. IEEE, 2012.
- J. H. Hubbell and S. M. Seltzer. Tables of x-ray mass attenuation coefficients and mass energy-absorption coefficients 1 kev to 20 mev for elements z= 1 to 92 and 48 additional substances of dosimetric interest. Technical report, National Inst. of Standards and Technology-PL, Gaithersburg, MD (United States). Ionizing Radiation Div., 1995. URL <https://physics.nist.gov/PhysRefData/XrayMassCoef/ComTab/water.html>.
- C. Huguen, J.-P. Foucher, J. Mascle, H. Ondréas, M. Thouement, S. Gontharet, A. Stadnitskaia, C. Pierre, G. Bayon, L. Loncke, et al. Menes caldera, a highly active site of brine seepage in the eastern mediterranean sea: “in situ” observations from the nautinil expedition (2003). *Marine Geology*, 261(1-4):138–152, 2009.
- N. Hurtós, X. Cufí, and J. Salvi. Calibration of optical camera coupled to acoustic multibeam for underwater 3d scene reconstruction. In *OCEANS'10 IEEE SYDNEY*, pages 1–7. IEEE, 2010.
- A. Isern and H. Clark. The ocean observatories initiative: A continued presence for interactive ocean research. *Marine Technology Society Journal*, 37(3), 2003.

- H. Ishaq and I. Dincer. A comparative evaluation of otec, solar and wind energy based systems for clean hydrogen production. *Journal of Cleaner Production*, 246: 118736, 2020.
- S. Ishibashi. The stereo vision system for an underwater vehicle. In *Oceans 2009-Europe*, pages 1–6. IEEE, 2009.
- A. J. Jamieson, B. Boorman, and D. O. Jones. Deep-sea benthic sampling. *Methods for the study of marine benthos*, pages 285–347, 2013.
- S. Jiang and R. C. Arkin. Mixed-initiative human-robot interaction: definition, taxonomy, and survey. In *2015 IEEE International conference on systems, man, and cybernetics*, pages 954–961. IEEE, 2015.
- S. J. Johnsen, D. Dahl-Jensen, N. Gundestrup, J. P. Steffensen, H. B. Clausen, H. Miller, V. Masson-Delmotte, A. E. Sveinbjörnsdóttir, and J. White. Oxygen isotope and palaeotemperature records from six greenland ice-core stations: Camp century, dye-3, grip, gisp2, renland and northgrip. *Journal of Quaternary Science: Published for the Quaternary Research Association*, 16(4):299–307, 2001.
- M. Kalaitzakis, B. Cain, S. Carroll, A. Ambrosi, C. Whitehead, and N. Vitzilaios. Fiducial markers for pose estimation: Overview, applications and experimental comparison of the artag, apriltag, aruco and stag markers. *Journal of Intelligent & Robotic Systems*, 101:1–26, 2021.
- D. J. Kalnicky and R. Singhvi. Field portable xrf analysis of environmental samples. *Journal of hazardous materials*, 83(1-2):93–122, 2001.
- K. Katija, E. Orenstein, B. Schlining, L. Lundsten, K. Barnard, G. Sainz, O. Boulaïs, M. Cromwell, E. Butler, B. Woodward, et al. Fathomnet: A global image database for enabling artificial intelligence in the ocean. *Scientific reports*, 12(1):15914, 2022.
- H. M. Khalid, L. W. Shiung, P. Nooralishahi, Z. Rasool, M. G. Helander, L. C. Kiong, and C. Ai-vyrn. Exploring psycho-physiological correlates to trust: Implications for human-robot-human interaction. In *Proceedings of the human factors and ergonomics society annual meeting*, volume 60, pages 697–701. SAGE Publications Sage CA: Los Angeles, CA, 2016.
- Z. Kopal. The measure of the moon. *Nature*, 211:127–128, 1966.
- R. Kraft, L. W. Beegle, E. Bulbul, G. Germain, R. P. Hodyss, S. Nulsen, G. Tremblay, and S. Vance. An x-ray fluorescence spectrometer for the europa lander. In *AGU Fall Meeting Abstracts*, volume 2018, pages P21E–3403, 2018.
- C. Kunz, C. Murphy, R. Camilli, H. Singh, J. Bailey, R. Eustice, M. Jakuba, K.-i. Nakamura, C. Roman, T. Sato, et al. Deep sea underwater robotic exploration in the ice-covered arctic ocean with auvs. In *2008 IEEE/RSJ International Conference on Intelligent Robots and Systems*, pages 3654–3660. IEEE, 2008.

- A. Laun. Artificial intelligence for the undersea system life cycle. In *OCEANS 2022, Hampton Roads*, pages 1–8. IEEE, 2022.
- N. Le Bris, P.-M. Sarradin, and S. Pennec. A new deep-sea probe for in situ ph measurement in the environment of hydrothermal vent biological communities. *Deep Sea Research Part I: Oceanographic Research Papers*, 48(8):1941–1951, 2001.
- Y. Li, L. Chen, K. P. Tee, and Q. Li. Reinforcement learning control for coordinated manipulation of multi-robots. *Neurocomputing*, 170:168–175, 2015.
- J. I. Lunine. Ocean worlds exploration. *Acta Astronautica*, 131:123–130, 2017.
- A. Mallios, P. Ridao, D. Ribas, M. Carreras, and R. Camilli. Toward autonomous exploration in confined underwater environments. *Journal of Field Robotics*, 33(7):994–1012, 2016.
- C. Martinez and P. Keener-Chavis. Noaa ship okeanos explorer: Telepresence in the service of science, education and outreach. In *OCEANS 2006*, pages 1–5. IEEE, 2006.
- P. A. McGillivray and V. Zykov. Ship-based cloud computing for advancing oceanographic research capabilities. In *OCEANS 2016 MTS/IEEE Monterey*, pages 1–7. IEEE, 2016.
- E. L. Meyer-Gutbrod, J. J. Pierson, and M. Behl. Community perspectives on justice, equity, diversity, and inclusion in ocean sciences. *Oceanography*, 36(1):67–73, 2023.
- E. Miguelanez, P. Patron, K. E. Brown, Y. R. Petillot, and D. M. Lane. Semantic knowledge-based framework to improve the situation awareness of autonomous underwater vehicles. *IEEE Transactions on Knowledge and Data Engineering*, 23(5):759–773, 2010.
- K. A. Miller, K. F. Thompson, P. Johnston, and D. Santillo. An overview of seabed mining including the current state of development, environmental impacts, and knowledge gaps. *Frontiers in Marine Science*, 4:418, 2018.
- R. C. Moeller, L. Jandura, K. Rosette, M. Robinson, J. Samuels, M. Silverman, K. Brown, E. Duffy, A. Yazzie, E. Jens, et al. The sampling and caching subsystem (scs) for the scientific exploration of jezero crater by the mars 2020 perseverance rover. *Space Science Reviews*, 217:1–43, 2021.
- S. A. Monk, A. Schaap, R. Hanz, S. M. Borisov, S. Loucaides, M. Arundell, S. Papadimitriou, J. Walk, D. Tong, J. Wyatt, et al. Detecting and mapping a co₂ plume with novel autonomous ph sensors on an underwater vehicle. *International Journal of Greenhouse Gas Control*, 112:103477, 2021.
- P. A. Montagna, J. G. Baguley, C.-Y. Hsiang, and M. G. Reuscher. Comparison of sampling methods for deep-sea infauna. *Limnology and oceanography: Methods*, 15(2):166–183, 2017.

- C. Mora, D. P. Tittensor, S. Adl, A. G. Simpson, and B. Worm. How many species are there on earth and in the ocean? *PLoS biology*, 9(8):e1001127, 2011.
- B. K. Muirhead, A. Nicholas, and J. Umland. Mars sample return mission concept status. In *2020 IEEE Aerospace Conference*, pages 1–8. IEEE, 2020.
- P. Muñoz, A. Cesta, A. Orlandini, and M. D. R-Moreno. Ogate: A framework for autonomous controllers assessment. *Robotics and Autonomous Systems*, 161: 104325, 2023.
- N. Muscettola, P. P. Nayak, B. Pell, and B. C. Williams. Remote agent: To boldly go where no ai system has gone before. *Artificial intelligence*, 103(1-2):5–47, 1998.
- A. Palomer, P. Ridao, D. Youakim, D. Ribas, J. Forest, and Y. Petillot. 3d laser scanner for underwater manipulation. *Sensors*, 18(4):1086, 2018.
- N. Palomeras, A. Penalver, M. Massot-Campos, G. Vallicrosa, P. L. Negre, J. J. Fernández, P. Ridao, P. J. Sanz, G. Oliver-Codina, and A. Palomer. I-auv docking and intervention in a subsea panel. In *2014 IEEE/RSJ international conference on intelligent robots and systems*, pages 2279–2285. IEEE, 2014.
- W. Paterson. Deformation within polar ice sheets: an analysis of the byrd station and camp century borehole-tilting measurements. *Cold Regions Science and Technology*, 8(2):165–179, 1983.
- C. Paull, S. Stratton, M. Conway, K. Brekke, T. C. Dawe, N. Maher, and W. Ussler. Deep sea vibracoring system improves rov sampling capability. *Eos, Transactions American Geophysical Union*, 82(30):325–326, 2001.
- A. Phung, G. Billings, A. Daniele, M. Walter, and R. Camilli. Partially automated robotic manipulation assisted by a shared autonomy framework for collaborative analysis and input from multiple remote scientists through natural language input and 3d scene understanding for real-time, in-situ elemental analysis. In *AGU Ocean Sciences Meeting*, 2022.
- P. M. Pilarski, M. R. Dawson, T. Degris, J. P. Carey, and R. S. Sutton. Dynamic switching and real-time machine learning for improved human control of assistive biomedical robots. In *2012 4th IEEE RAS & EMBS International Conference on Biomedical Robotics and Biomechatronics (BioRob)*, pages 296–302. IEEE, 2012.
- C. Pohl, K. Hitzler, R. Grimm, A. Zea, U. D. Hanebeck, and T. Asfour. Affordance-based grasping and manipulation in real world applications. In *2020 IEEE/RSJ International Conference on Intelligent Robots and Systems (IROS)*, pages 9569–9576. IEEE, 2020.
- M. Prats, J. Garcia, S. Wirth, D. Ribas, P. Sanz, P. Ridao, N. Gracias, and G. Oliver. Multipurpose autonomous underwater intervention: A systems integration perspective. In *2012 20th Mediterranean Conference on Control & Automation (MED)*, pages 1379–1384. IEEE, 2012.

- N. Raineault. New frontiers in ocean exploration: The e/v nautilus, noaa ship okeanos explorer, and r/v falkor 2018 field season. 2019.
- E. Ramirez-Llodra, A. Brandt, R. Danovaro, B. De Mol, E. Escobar, C. R. German, L. A. Levin, P. Martinez Arbizu, L. Menot, P. Buhl-Mortensen, et al. Deep, diverse and definitely different: unique attributes of the world’s largest ecosystem. *Biogeosciences*, 7(9):2851–2899, 2010.
- A. Ratsimandresy, S. Donnet, P. Goulet, R. Bachmayer, and B. Claus. Variation in the structure of the water column as captured by slocum glider ctd and by ctd from a research vessel and assessment of internal waves. In *2014 Oceans-St. John’s*, pages 1–10. IEEE, 2014.
- C. M. Reddy, J. S. Arey, J. S. Seewald, S. P. Sylva, K. L. Lemkau, R. K. Nelson, C. A. Carmichael, C. P. McIntyre, J. Fenwick, G. T. Ventura, et al. Composition and fate of gas and oil released to the water column during the deepwater horizon oil spill. *Proceedings of the National Academy of Sciences*, 109(50):20229–20234, 2012.
- C. Rees, L. Pender, K. Sherrin, C. Schwanger, P. Hughes, S. Tibben, A. Marouchos, and M. Rayner. Methods for reproducible shipboard sfa nutrient measurement using rmns and automated data processing. *Limnology and Oceanography: Methods*, 17(1):25–41, 2019.
- D. Ribas, N. Palomeras, P. Ridao, M. Carreras, and A. Mallios. Girona 500 auv: From survey to intervention. *IEEE/ASME Transactions on mechatronics*, 17(1):46–53, 2011.
- A. Roncone, O. Mangin, and B. Scassellati. Transparent role assignment and task allocation in human robot collaboration. In *2017 IEEE International Conference on Robotics and Automation (ICRA)*, pages 1014–1021. IEEE, 2017.
- D. K. Rout, B. N. Subudhi, T. Veerakumar, and S. Chaudhury. Spatio-contextual gaussian mixture model for local change detection in underwater video. *Expert Systems with Applications*, 97:117–136, 2018.
- M. J. Schuster, M. G. Müller, S. G. Brunner, H. Lehner, P. Lehner, R. Sakagami, A. Dömel, L. Meyer, B. Vodermayer, R. Giubilato, et al. The arches space-analogue demonstration mission: Towards heterogeneous teams of autonomous robots for collaborative scientific sampling in planetary exploration. *IEEE Robotics and Automation Letters*, 5(4):5315–5322, 2020.
- D. J. Segelstein. *The complex refractive index of water*. PhD thesis, University of Missouri–Kansas City, 1981. URL <http://omlc.ogi.edu/spectra/water/data/segelstein81.dat>.
- A. Settimi, C. Pavan, V. Varricchio, M. Ferrati, E. Mingo Hoffman, A. Rocchi, K. Melo, N. G. Tsagarakis, and A. Bicchi. A modular approach for remote operation

- of humanoid robots in search and rescue scenarios. In *Modelling and Simulation for Autonomous Systems: First International Workshop, MESAS 2014, Rome, Italy, May 5-6, 2014, Revised Selected Papers 1*, pages 192–205. Springer, 2014.
- S. Shefsky. Comparing field portable x-ray fluorescence (xrf) to laboratory analysis of heavy metals in soil. In *International symposium of field screening methods for hazardous wastes and toxic chemicals, Las Vegas, Nevada, USA*, 1997.
- E. Simetti. Autonomous underwater intervention. *Current Robotics Reports*, 1:117–122, 2020.
- A. Singh, S. H. Seo, Y. Hashish, M. Nakane, J. E. Young, and A. Bunt. An interface for remote robotic manipulator control that reduces task load and fatigue. In *2013 IEEE RO-MAN*, pages 738–743. IEEE, 2013.
- S. Singh, S. E. Webster, L. Freitag, L. L. Whitcomb, K. Ball, J. Bailey, and C. Taylor. Acoustic communication performance of the whoi micro-modem in sea trials of the nereus vehicle to 11,000 m depth. In *OCEANS 2009*, pages 1–6. IEEE, 2009.
- S. Siroouspour and P. Setoodeh. Multi-operator/multi-robot teleoperation: an adaptive nonlinear control approach. In *2005 IEEE/RSJ International Conference on Intelligent Robots and Systems*, pages 1576–1581. IEEE, 2005.
- S. Sivčev, J. Coleman, E. Omerdić, G. Dooly, and D. Toal. Underwater manipulators: A review. *Ocean engineering*, 163:431–450, 2018.
- P. A. Skoglund Lindberg. *Electron-Impact Liquid-Jet Water-Window X-ray Sources*. PhD thesis, Universitetsservice US AB, 2010.
- C. Smith, Y. Karayiannidis, L. Nalpantidis, X. Gratal, P. Qi, D. V. Dimarogonas, and D. Kragic. Dual arm manipulation—a survey. *Robotics and Autonomous systems*, 60(10):1340–1353, 2012.
- M. C. Smith, M. R. Perfit, and I. R. Jonasson. Petrology and geochemistry of basalts from the southern juan de fuca ridge: Controls on the spatial and temporal evolution of mid-ocean ridge basalt. *Journal of Geophysical Research: Solid Earth*, 99 (B3):4787–4812, 1994.
- S. R. Smith, M. A. Bourassa, J. Elya, T. Huang, K. M. Gill, F. R. Greguska III, N. T. Chung, V. Tsontos, B. Holt, T. Cram, et al. The distributed oceanographic match-up service. *Big Data Analytics in Earth, Atmospheric, and Ocean Sciences*, pages 189–214, 2022.
- P. P. Soares, L. B. de Souza, M. Mendonça, R. H. Palácios, and J. P. L. S. de Almeida. Group of robots inspired by swarm robotics exploring unknown environments. In *2018 IEEE international conference on fuzzy systems (FUZZ-IEEE)*, pages 1–7. IEEE, 2018.

- L. J. Stal. Microbial mats in coastal environments. In *Microbial mats: structure, development and environmental significance*, pages 21–32. Springer, 1994.
- M. Stallard, S. Apitz, and C. Dooley. X-ray fluorescence spectrometry for field analysis of metals in marine sediments. *Marine Pollution Bulletin*, 31(4-12):297–305, 1995.
- E. R. Stofan, C. Elachi, J. I. Lunine, R. D. Lorenz, B. Stiles, K. Mitchell, S. Ostro, L. Soderblom, C. Wood, H. Zebker, et al. The lakes of titan. *Nature*, 445(7123):61–64, 2007.
- K. Szocik and M. Braddock. Why human enhancement is necessary for successful human deep-space missions. *The New Bioethics*, 25(4):295–317, 2019.
- T. Takahashi, S. Yoshino, Y. Takaya, T. Nozaki, K. Ohki, T. Ohki, T. Sakka, and B. Thornton. Quantitative in situ mapping of elements in deep-sea hydrothermal vents using laser-induced breakdown spectroscopy and multivariate analysis. *Deep Sea Research Part I: Oceanographic Research Papers*, 158:103232, 2020.
- A. K. Tanwani and S. Calinon. A generative model for intention recognition and manipulation assistance in teleoperation. In *2017 IEEE/RSJ International Conference on Intelligent Robots and Systems (IROS)*, pages 43–50. IEEE, 2017.
- N. Tarcea, T. Frosch, P. Rösch, M. Hilchenbach, T. Stuffler, S. Hofer, H. Thiele, R. Hochleitner, and J. Popp. Raman spectroscopy—a powerful tool for in situ planetary science. *Strategies of life detection*, pages 281–292, 2008.
- J. Teague, M. J. Allen, and T. B. Scott. The potential of low-cost rov for use in deep-sea mineral, ore prospecting and monitoring. *Ocean Engineering*, 147:333–339, 2018.
- S. Tellex, N. Gopalan, H. Kress-Gazit, and C. Matuszek. Robots that use language. *Annual Review of Control, Robotics, and Autonomous Systems*, 3:25–55, 2020.
- A. Thobbi, Y. Gu, and W. Sheng. Using human motion estimation for human-robot cooperative manipulation. In *2011 IEEE/RSJ International Conference on Intelligent Robots and Systems*, pages 2873–2878. IEEE, 2011.
- T. Thorsnes, O. A. Misund, and M. Smelror. Seabed mapping in norwegian waters: programmes, technologies and future advances. *Geological Society, London, Special Publications*, 499(1):99–118, 2020.
- G. A. Trobbiani, A. Irigoyen, L. A. Venerus, P. Fiorda, and A. M. Parma. A low-cost towed video camera system for underwater surveys: comparative performance with standard methodology. *Environmental monitoring and assessment*, 190:1–12, 2018.
- E. Turan, S. Speretta, and E. Gill. Autonomous navigation for deep space small satellites: Scientific and technological advances. *Acta Astronautica*, 2022.

- C. L. Van Dover. Tighten regulations on deep-sea mining. *Nature*, 470(7332):31–33, 2011.
- B. Varga, S. Meier, S. Schwab, and S. Hohmann. Model predictive control and trajectory optimization of large vehicle-manipulators. In *2019 IEEE International Conference on Mechatronics (ICM)*, volume 1, pages 60–66. IEEE, 2019.
- P. Vrolijk, L. Summa, B. Ayton, P. Nomikou, A. Hüpers, F. Kinnaman, S. Sylva, D. Valentine, and R. Camilli. Using a ladder of seeps with computer decision processes to explore for and evaluate cold seeps on the costa rica active margin. *Frontiers in Earth Science*, 9:601019, 2021.
- J. Wang and E. Olson. Apriltag 2: Efficient and robust fiducial detection. In *2016 IEEE/RSJ International Conference on Intelligent Robots and Systems (IROS)*, pages 4193–4198. IEEE, 2016.
- K. Wien, D. Wissmann, M. Kölling, and H. D. Schulz. Fast application of x-ray fluorescence spectrometry aboard ship: how good is the new portable spectro xepos analyser? *Geo-Marine Letters*, 25:248–264, 2005.
- S. B. Williams, O. Pizarro, M. Jakuba, and N. Barrett. Auv benthic habitat mapping in south eastern tasmania. In *Field and Service Robotics: Results of the 7th International Conference*, pages 275–284. Springer, 2010.
- A. Witze et al. Nasa’s mars rover makes ‘fantastic’find in search for past life. *Nature*, 609(7929):885–886, 2022.
- N. Wogman and K. Nielson. Development and application of an in situ x-ray fluorescence spectrometer for underwater sediment analysis. *Environment International*, 4(4):313–324, 1980.
- C. Wong, E. Yang, X.-T. Yan, and D. Gu. Autonomous robots for harsh environments: a holistic overview of current solutions and ongoing challenges. *Systems Science & Control Engineering*, 6(1):213–219, 2018.
- M. Wonsick and T. Padir. A systematic review of virtual reality interfaces for controlling and interacting with robots. *Applied Sciences*, 10(24):9051, 2020.
- R. B. Wynn, V. A. Huvenne, T. P. Le Bas, B. J. Murton, D. P. Connelly, B. J. Bett, H. A. Ruhl, K. J. Morris, J. Peakall, D. R. Parsons, et al. Autonomous underwater vehicles (auvs): Their past, present and future contributions to the advancement of marine geoscience. *Marine geology*, 352:451–468, 2014.
- Z. Xian, P. Lertkultanon, and Q.-C. Pham. Closed-chain manipulation of large objects by multi-arm robotic systems. *IEEE Robotics and Automation Letters*, 2(4):1832–1839, 2017.

- E. You and K. Hauser. Assisted teleoperation strategies for aggressively controlling a robot arm with 2d input. In *Robotics: science and systems*, volume 7, page 354. MIT Press USA, 2012.
- J. Zhao, J. O. Wallgrün, P. C. LaFemina, J. Normandeau, and A. Klippel. Harnessing the power of immersive virtual reality-visualization and analysis of 3d earth science data sets. *Geo-spatial Information Science*, 22(4):237–250, 2019.
- M. Zucker, J. Kuffner, and M. Branicky. Multipartite rrt_s for rapid replanning in dynamic environments. In *Proceedings 2007 IEEE International Conference on Robotics and Automation*, pages 1603–1609. IEEE, 2007.